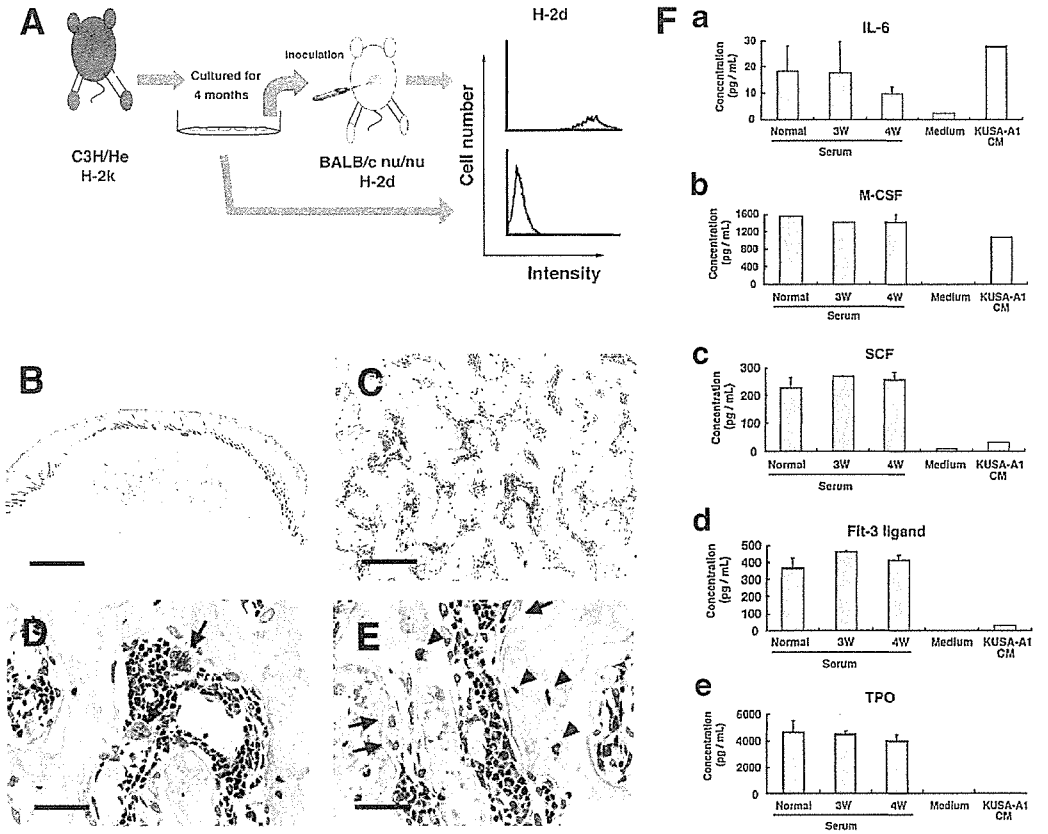

Fig. 3. Hematopoietic cells of host origin in the ectopic bone and serum levels of cytokines after subcutaneous implantation of KUSA-A1 cells. **A**: Flow cytometric analysis of the H-2d antigen in the hematopoietic cells of ectopic bone and KUSA-A1 cells in vitro. The hematopoietic cells in KUSA-A1 bone were examined for expression of the H-2d antigen of the host mice. **B–E**: Histopathological appearance of the hematopoietic cells used for flow cytometric analysis. Trilineage cells, that is, megakaryocytes (D, arrows), erythroblasts (D, E), and granulocytes (E), were observed. Osteoblasts and mature osteocytes are indicated by arrows and arrowheads, respectively (E). Scale bars: 2 mm (B), 400 μm (C), 100 μm (D, E). **F**: Serum levels of interleukin-6 (IL-6) (**a**), macrophage-colony stimulating factor (M-CSF) (**b**), stem cell factor (SCF) (**c**), fms-like tyrosine kinase-3 (Flt-3) ligand (**d**), and thrombopoietin (TPO) (**e**), measured by the ELISA method. The blood samples were obtained at 5 weeks after implantation.

increases in the HSC population. In the HSC population, both the CFU-S and KSL cells increased. The niche that regulates the generation and differentiation of the HSCs was formed following KUSA-A1 cell implantation, and subsequent membranous ossification in vivo. The enlarged area of niche, that is, the inner surface of bone during the dynamic process of membranous osteogenesis may account for the dramatic upregulation of HSCs in the host bone marrow. Once the osteogenic process is terminated, the number of osteoclasts decreases and no bone is remodeled. Furthermore, the number of the KSL cells returns to the basal level in host bone marrow. These facts suggest a correlation between the osteogenic process (Fig. 1C) and increasing number of KSL cells (Fig. 4F).

The source of the CFU-S in the peripheral blood of the mice implanted with KUSA-A1 osteoblasts may be the bone marrow of (a) the ectopic bone; (b) the host femur; (c) both the ectopic bone and the host femur (Fig. 4C). Mobilization of CFU-S from ectopic bone into the peripheral blood is the most likely cause since the induction of HSCs was accompanied by dynamic osteogenesis. The increased HSC number in the host bone marrow can be explained by HSC mobilization from ectopic bone into the peripheral blood. In the normal mice, such migration or mobilization of hematopoietic cells occurs during development. Hematopoietic events in the mouse begin in the yolk sac and aorta-gonad-mesonephros region at day 7 of gestation, and they shift the site to the fetal liver at mid-gestation followed by the bone marrow shortly before birth. The prevailing notion has been that this sequence reflects the migration of HSCs from the yolk sac to the definitive hematopoietic sites. Observation in this study, that is, the generation of ectopic bone in the subcutaneous tissues and the resultant migration of HSCs via the peripheral blood, seems to mimic above process during developments (Dzierzak et al., 1998).

Unexpected upregulation of MHC antigen after implantation of donor cells

Although most HSCs have been reported to express MHCs, that is, HLA in humans, and H-2 antigens in mice, no mesenchymal stem cells have been reported to express MHC antigens at least in vitro (Jiang et al., 2002). Since lack of these antigens on the cell surface may contribute to the induction of tolerance in these cells when transplanted in allogeneic combination, the complete rejection of the transplanted mesenchymal cells and de novo expression of the H-2 antigen after in vivo implantation was contrary to our expectation. We do not know the molecular mechanisms responsible for upregulated expression of H-2 and downregulated expression of Sca-1 after cell implantation, but care should be exercised when mesenchymal cells are implanted for therapeutic purposes, because membrane-bound molecules, including functionally essential molecules, might be modulated after implantation.

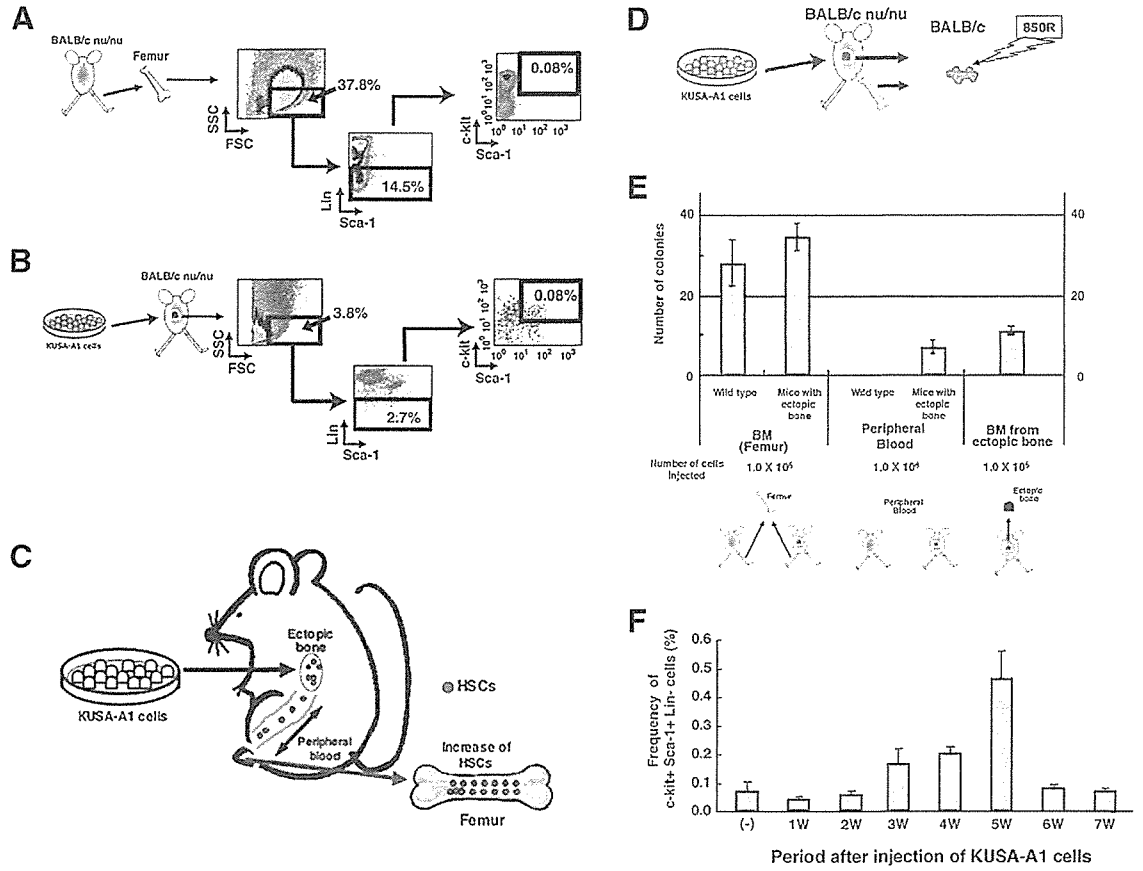

Fig. 4. Mobilization of c-kit$^+$ Sca-1$^+$ Lin$^-$ (KSL) cells in the ectopic bones generated by KUSA-A1 cells. **A** and **B**: Flow cytometric analysis of hematopoietic stem cell markers was performed on hematopoietic cells in the femur of BALB/c nu/nu mice (A) and the ectopic bone generated in BALB/c nu/nu mice (B). KSL cells accounted for 0.08% of the hematopoietic cells in KUSA-A1 bone. **C**: Proposed mechanism of HSC mobilization in the peripheral blood of mice with the ectopic bone, and the increased HSCs in the femur of mice implanted with osteoblasts. Osteoblastic cells whose number has been increased by local injection into the tissues support an increase in number of HSCs in both bone marrow and peripheral blood, as a result of an increase in size of the microenvironment or niche in vivo. The niche size defined by dynamic osteogenic process affects the number of stem cells. **D**: Experimental design to investigate mobilization of CFU-S in the peripheral blood of mice with the ectopic bone, and the proportion of KSL cells in the femur of mice implanted with KUSA-A1 cells. Hematopoiesis was induced in the ectopic bone by KUSA-A1 cell implantation (See Fig. 3). The hematopoietic cells in the ectopic bone and the host femur were analyzed for further CFU-S analysis in mice exposed to 850 cGy irradiation. **E**: CFU-S assay in the marrow cells of the femur of mice not implanted with any cells; the femoral marrow cells of mice with ectopic bone; peripheral blood cells of mice not implanted with cells; peripheral blood cells of mice with ectopic bone; marrow cells in ectopic bone. The blood samples were obtained at 5 weeks after implantation. The number of HSC or CFU-s increased to $11.2 \pm 0.8/1.0 \times 10^5$ cells in the KUSA-A1-induced ectopic bone. CFU-s in the peripheral blood increased to $7.0 \pm 1.7/10^6$ cells at day 12 after implantation of the KUSA-A1 cells while no CFU-s were detected in the peripheral blood from mice without cell implantation. **F**: Time course of the proportion of KLS cells in the femur of mice implanted with KUSA-A1 cells.

Crucial role of marrow stromal subsets in HSC regulation

HSCs are a subset of bone marrow cells that are capable of self-renewal and of forming all types of blood cells. The increases in bone size generated by the spindle-shaped KUSA-A1 osteoblasts correlated with the increase in the number of HSCs. The osteoblasts and a subpopulation of the HSCs expressed N-cadherin, a cell-surface molecule that helps cells adhere to one another, and N-cadherin and -catenin may form important components of the interaction between HSCs and their niche (Zhang et al., 2003). The Notch signaling pathway is also known to regulate cell-fate decisions in many organisms (Calvi et al., 2003). Involvement of cytokine signaling in HSC regulation has been reported to be crucial to the development of blood-forming tissue in embryos. The doubling of bone size mirrored the increase in the HSC population in the mice implanted with KUSA-A1 cells.

The strategy to increase the size of the HSC population by implanting osteoblasts into the subcutaneous tissue to increase the osteoblast cell population may be proven to be of certain clinical value in the future. The concept that a microenvironment or niche controls HSCs may be useful for HSC expansion in vivo, and has potential implications for HSC harvesting and recovery after transplantation (Fig. 4C). Direct implantation of KUSA-A1 cells into syngeneic or immunodeficient mice, in order to better understand the interactions between HSCs and bone marrow, may therefore lead to the development of practical methods of manipulating stem cells and define a model for investigating the impact of the microenvironment on cell physiology (Li et al., 2000). Cellular and molecular identification using the strategy of niche-constituent cells or signaling pathways will provide pharmacological targets with therapeutic potential for stem-cell-based therapies.

ACKNOWLEDGMENTS

This study was supported by a grant from the Ministry of Education, Culture, Sports, Science, and Technology (MEXT) of Japan and the Health and Labour Sciences Research Grants, and the Pharmaceuticals and Medical

Devices Agency to A. U. We thank T. Tsurumi and T. Shimizu for their excellent technical assistance in animal and cell culture.

LITERATURE CITED

Calvi LM, Adams GB, Weibrecht KW, Weber JM, Olson DP, Knight MC, Martin RP, Schipani E, Divieti P, Bringhurst FR, Milner LA, Kronenberg HM, Scadden DT. 2003. Osteoblastic cells regulate the haematopoietic stem cell niche. Nature 425:841–846.

Dzierzak E, Medvinsky A, de Bruijn M. 1998. Qualitative and quantitative aspects of haematopoietic cell development in the mammalian embryo. Immunol Today 19:228–236.

Goodell MA, Brose K, Paradis G, Conner AS, Mulligan RC. 1996. Isolation and functional properties of murine hematopoietic stem cells that are replicating in vivo. J Exp Med 183:1797–1806.

Harrison DE, Russell ES. 1972. The response of W-W v and Sl-Sl d anaemic mice to haemopoietic stimuli. Br J Haematol 22:155–168.

Ikehara S. 2000. Pluripotent hemopoietic stem cells in mice and humans. Proc Soc Exp Biol Med 223:149–155.

Jiang Y, Jahagirdar BN, Reinhardt RL, Schwartz RE, Keene CD, Ortiz-Gonzalez XR, Reyes M, Lenvik T, Lund T, Blackstad M, Du J, Aldrich S, Lisberg A, Low WC, Largaespada DA, Verfaillie CM. 2002. Pluripotency of mesenchymal stem cells derived from adult marrow. Nature 418:41–49.

Kohyama J, Abe H, Shimazaki T, Koizumi A, Nakashima K, Gojo S, Taga T, Okano H, Hata J, Umezawa A. 2001. Brain from bone: Efficient "meta-differentiation" of marrow stroma-derived mature osteoblasts to neurons with Noggin or a demethylating agent. Differentiation 68:235–244.

Li Y, Hisha H, Inaba M, Lian Z, Yu C, Kawamura M, Yamamoto Y, Nishio N, Toki J, Fan H, Ikehara S. 2000. Evidence for migration of donor bone marrow stromal cells into recipient thymus after bone marrow transplantation plus bone grafts: A role of stromal cells in positive selection. Exp Hematol 28:950–960.

Lord BI. 1990. The architecture of bone marrow cell populations. Int J Cell Cloning 8:317–331.

Makino S, Fukuda K, Miyoshi S, Konishi F, Kodama H, Pan J, Sano M, Takahashi T, Hori S, Abe H, Hata J, Umezawa A, Ogawa S. 1999. Cardiomyocytes can be generated from marrow stromal cells in vitro. J Clin Invest 103:697–705.

Matsuzaki Y, Kinjo K, Mulligan RC, Okano H. 2004. Unexpectedly efficient homing capacity of purified murine hematopoietic stem cells. Immunity 20: 87–93.

Mori T, Kiyono T, Imabayashi H, Takeda Y, Tsuchiya K, Miyoshi S, Makino H, Matsumoto K, Saito H, Ogawa S, Sakamoto M, Hata J-I, Umezawa A. 2005. Combination of hTERT and Bmi-1, E6 or E7 induce prolongation of the life span of bone marrow stromal cells from an elderly donor without affecting their neurogenic potential. Mol Cell Biol 25:5183–5195.

Okada S, Nakauchi H, Nagayoshi K, Nishikawa S, Miura Y, Suda T. 1991. Enrichment and characterization of murine hematopoietic stem cells that express c-kit molecule. Blood 78:1706–1712.

Okada S, Nakauchi H, Nagayoshi K, Nishikawa S, Miura Y, Suda T. 1992. In vivo and in vitro stem cell function of c-kit- and Sca-1-positive murine hematopoietic cells. Blood 80:3044–3050.

Osawa M, Hanada K, Hamada H, Nakauchi H. 1996. Long-term lymphohematopoietic reconstitution by a single CD34-low/negative hematopoietic stem cell. Science 273:242–245.

Pittenger MF, Mackay AM, Beck SC, Jaiswal RK, Douglas R, Mosca JD, Moorman MA, Simonetti DW, Craig S, Marshak DR. 1999. Multilineage potential of adult human mesenchymal stem cells. Science 284:143–147.

Schöfield R. 1978. The relationship between the spleen colony-forming cell and the haemopoietic stem cell. Blood Cells 4:7–25.

Sharov AA, Piao Y, Matoba R, Dudekula DB, Qian Y, VanBuren V, Falco G, Martin PR, Stagg CA, Bassey UC, Wang Y, Carter MG, Hamatani T, Aiba K, Akutsu H, Sharova L, Tanaka TS, Kimber WL, Yoshikawa T, Jaradat SA, Pantano S, Nagaraja R, Boheler KR, Taub D, Hodes RJ, Longo DL, Schlessinger D, Keller J, Klotz E, Kelsoe G, Umezawa A, Vescovi AL, Rossant J, Kunath T, Hogan BL, Curci A, D'Urso M, Kelso J, Hide W, Ko MS. 2003. Transcriptome analysis of mouse stem cells and early embryos. PLoS Biol 1:E74.

Siminovitch L, McCulloch EA, Till JE. 1963. The distribution of colony-forming cells among spleen colonies. J Cell Physiol 62:327–336.

Spangrude GJ, Heimfeld S, Weissman IL. 1988. Purification and characterization of mouse hematopoietic stem cells. Science 241:58–62.

Takeda Y, Mori T, Imabayashi H, Kiyono T, Gojo S, Miyoshi S, Hida N, Ita M, Segawa K, Ogawa S, Sakamoto M, Nakamura S, Umezawa A. 2004. Can the life span of human marrow stromal cells be prolonged by bmi-1, E6, E7, and/or telomerase without affecting cardiomyogenic differentiation? J Gene Med 6:833–845.

Terai M, Uyama T, Sugiki T, Li XK, Umezawa A, Kiyono T. 2005. Immortalization of human fetal cells: the life span of umbilical cord blood-derived cells can be prolonged without manipulating p16INK4a/RB braking pathway. Mol Biol Cell 16:1491–1499.

Till JE, McCulloch CE. 1961. A direct measurement of the radiation sensitivity of normal mouse bone marrow cells. Radiat Res 14:213–222.

Till JE, McCulloch EA, Siminovitch L. 1964. A stochastic model of stem cell proliferation, based on the growth of spleen colony-forming cells. Proc Natl Acad Sci USA 51:29–36.

Umezawa A, Maruyama T, Segawa K, Shadduck RK, Waheed A, Hata J. 1992. Multipotent marrow stromal cell line is able to induce hematopoiesis in vivo. J Cell Physiol 151:197–205.

Watt FM, Hogan BL. 2000. Out of Eden: Stem cells and their niches. Science 287:1427–1430.

Weissman IL. 2000. Stem cells: Units of development, units of regeneration, and units in evolution. Cell 100:157–168.

Yoshimoto M, Shinohara T, Heike T, Shiota M, Kanatsu-Shinohara M, Nakahata T. 2003. Direct visualization of transplanted hematopoietic cell reconstitution in intact mouse organs indicates the presence of a niche. Exp Hematol 31: 733–740.

Zhang J, Niu C, Ye L, Huang H, He X, Tong WG, Ross J, Haug J, Johnson T, Feng JQ, Harris S, Wiedemann LM, Mishina Y, Li L. 2003. Identification of the haematopoietic stem cell niche and control of the niche size. Nature 425: 836–841.

0013-7227/06/$15.00/0
Printed in U.S.A.

Endocrinology 147(9):4104–4111

doi: 10.1210/en.2006-0162

Differentiation of Adult Stem Cells Derived from Bone Marrow Stroma into Leydig or Adrenocortical Cells

Takashi Yazawa, Tetsuya Mizutani, Kazuya Yamada, Hiroko Kawata, Toshio Sekiguchi, Miki Yoshino, Takashi Kajitani, Zhangfei Shou, Akihiro Umezawa, and Kaoru Miyamoto

Department of Biochemistry (T.Y., T.M., K.Y., H.K., T.S., M.Y., T.K., Z.S., K.M.), Faculty of Medical Sciences, University of Fukui, Fukui 910-1193, Japan; Core Research for Evolutional Science and Technology (T.Y., T.M., K.Y., H.K., T.S., M.Y., T.K., Z.S., K.M.), Japan Science and Technology Agency, Saitama 332-0012, Japan; and National Research Institute for Child Health and Development (A.U.), Tokyo 157-8535, Japan

Adult stem cells from bone marrow, referred to as mesenchymal stem cells or marrow stromal cells (MSCs), are defined as pluripotent cells and have the ability to differentiate into multiple mesodermal cells. In this study, we investigated whether MSCs from rat, mouse, and human are able to differentiate into steroidogenic cells. When transplanted into immature rat testes, adherent marrow-derived cells (including MSCs) were found to be engrafted and differentiate into steroidogenic cells that were indistinguishable from Leydig cells. Isolated murine MSCs transfected with green fluorescence protein driven by the promoter of P450 side-chain cleaving enzyme gene (CYP11A), a steroidogenic cell-specific gene, were used to detect steroidogenic cell production *in vitro*. During *in vitro* differentiation, green fluorescence protein-positive cells, which had characteristics similar to those of Leydig cells, were found. Stable transfection of murine MSCs with a transcription factor, steroidogenic factor-1, followed by treatment with cAMP almost recapitulated the properties of Leydig cells, including the production of testosterone. Transfection of human MSCs with steroidogenic factor-1 also led to their conversion to steroidogenic cells, but they appeared to be glucocorticoid- rather than testosterone-producing cells. These results indicate that MSCs represent a useful source of stem cells for producing steroidogenic cells that may provide basis for their use in cell and gene therapy. (*Endocrinology* 147: 4104–4111, 2006)

STEM CELLS ARE self-renewing elements with the capacity to generate multiple distinct cell lineages. They exist in various tissues, even in adults, and have been isolated from a variety of differentiated tissues, including bone marrow, umbilical blood, brain, and fat (1–6). Among these, bone marrow-derived mesenchymal stem cells (MSCs), also known as marrow stromal cells, are defined as pluripotent cells and have been shown to differentiate into adipocytes, chondrocytes, osteoblasts, and hematopoietic-supporting stroma both *in vivo* and *ex vivo* (1–3). Furthermore, they are able to generate cells of all three germ layers (7, 8). In addition to their multipotency for differentiation, MSCs have attracted considerable interest for use in cell and gene therapy because these cells can easily be obtained from adult marrow tissue (8–10).

The gonad and adrenal gland are the primary steroidogenic organs in mammals. In the gonad, male Leydig cells or female granulosa and theca cells are responsible for the production of androgens and estrogens. The adrenal cortex produces glucocorticoids and mineralocorticoids, although some androgens are also produced in many species, except rodents. These steroidogenic organs develop from the common adrenogenital primodium, which originates from the intermediate mesoderm (11). Fetal-type steroidogenic cells appear when the adrenogenital primodium differentiates into the adrenal cortex and the gonads of the two sexes. These are replaced by adult-type steroidogenic cells during the period between birth and puberty (12, 13), but these processes are poorly understood.

One approach to resolving the complexities of organogenesis is to use stem cells as a model system for differentiation. In this study, the differentiation of MSCs into steroidogenic cells was examined *in vivo* and *in vitro* by several methods. A number of studies have reported that the injection of MSCs into some tissues leads to the differentiation of the injected cells into tissue-specific cells, probably due to the microenvironment near the injection sites. To determine whether MSCs are able to differentiate into steroidogenic cells, we injected a purified population of rat MSCs into the prepubertal rat testis and examined the fate of these cells by immunohistochemistry. In addition, the spontaneous differentiation of MSCs to specific cells can be monitored by the expression of specific genes in the differentiated cells. One such experimental approach, known as a promoter-sorting method, is to use fluorescence-activated cell sorting (FACS) to select green fluorescence protein (GFP)-positive MSCs in which the expression of GFP is under the control of the promoter of a gene that is expressed in a cell type-specific fashion. In this study, to demonstrate the emergence of steroidogenic cells from isolated MSCs *in vitro*, a GFP expression vector driven by the CYP11A promoter (CYP11A is a

First Published Online May 25, 2006

Abbreviations: ES, Embryonic stem; FACS, fluorescence activated cell sorting; GFP, green fluorescence protein; hMSC, human MSC; 3β-HSD I, 3β-hydroxysteroid dehydrogenase I; 17β-HSD III, 17β-hydroxysteroid dehydrogenase III; mMSC, murine MSC; MSC, mesenchymal stem cell; P450arom, cytochrome P450 aromatase; P450c17, cytochrome P450 17α-hydroxylase; P450c21, cytochrome P450 steroid 21-hydroxylase; P450scc, P450 side-chain cleaving enzyme; SF, steroidogenic factor; StAR, steroidogenic acute regulatory protein.

Endocrinology is published monthly by The Endocrine Society (http://www.endo-society.org), the foremost professional society serving the endocrine community.

gene encoding the cholesterol side-chain cleavage enzyme, an essential enzyme for steroidogenesis) was integrated into the MSCs, and GFP-positive MSCs were then separated by fluorocytometry. Finally, to achieve the efficient differentiation of the isolated MSCs *in vitro*, the orphan nuclear receptor, steroidogenic factor (SF)-1 was ectopically expressed in MSCs. MSCs successfully differentiated into steroidogenic cells using any of these procedures. These results indicate that MSCs represent a useful source of stem cells for producing steroidogenic cells that may provide basis for their use in cell and gene therapy.

Materials and Methods

Animals

GFP transgenic rats [SD TgN(act-EGFP)OsbCZ-004] were kindly provided by Dr. M. Okabe (Osaka University, Osaka, Japan). Sprague Dawley rats were purchased from Sankyo (Shizuoka, Japan). At all times, the animals were treated according to National Institutes of Health guidelines. The donor animals used in this study were generally 4–5 wk old, and the recipient animals were 3 wk old.

Histology and immunofluorescence analysis

Immunohisto- and cytochemical staining with antirat P450 side-chain cleaving enzyme (P450scc) (C-16; Santa Cruz Biotechnology, Santa Cruz, CA), antimouse 3β-hydroxysteroid dehydrogenase I (3β-HSD I) (kindly provided by Dr. A. Payne, Stanford University Medical Center, Stanford, CA), antipig cytochrome P450 17 α-hydroxylase (P450c17) (kindly provide by Dr. D. Hales, University of Illinois at Chicago, Chicago, IL) or anti-GFP (Medical & Biological Laboratories Co., Ltd.) were performed on 10-μm frozen sections or cultured cells on glass slides using standard protocols. Appropriate Cy3- or fluorescein isothiocyanate-conjugated secondary antibodies (Sigma, St. Louis, MO) were used for detection.

Cell culture, stable transfection, and hormone assay

MSCs from GFP transgenic rats were collected and cultured as described by Pochampally *et al.* (14). Mouse (KUM9) (15) or human (hMSC-hTERT-E6/E7) (16) bone marrow-derived MSCs were maintained in Iscova's MEM or DMEM with 10% fetal calf serum. Plasmid DNA was transfected using the LipofectAmine PLUS reagent (Invitrogen, Carlsbad, CA) or calcium phosphate coprecipitation. Cells were used for the experiments after 10–12 passages, and steroid hormone production was sustained for at least 4 months. The levels of each steroid hormone in the media were measured by RIA.

Transplantation

Bone marrow cells from TgN(ActbEGFP) transgenic rats (1×10^6) were injected into the testes of 3-wk-old SD rats. Two to three weeks after transplantation, testes were removed to examine histochemically survival and differentiation of transplanted cells.

Plasmid construction

A 2.3-kb fragment of the human CYP11A (P450scc gene) promoter that functions specifically in steroidogenic organs (17) was obtained by PCR using pSCC2300-LacZ (kindly provided by Dr. B. C. Chung, Institute of Molecular Biology, Taipei, Taiwan) as a template and integrated into a promoter-less pEGFP-1 vector (CLONTECH, Palo Alto, CA). The *Eco*RI-*Stu*I restriction fragment, containing the CYP11A promoter-GFP, was then excised and inserted into *Eco*RI and *Swa*I site of pPUR (CLONTECH). The expression vector for rat SF-1 cDNA containing the entire coding region was generated by RT-PCR and subcloned into pIRES-puro2 vector (CLONTECH).

FACS analysis and cell purification

Cells were harvested by treatment with 0.25% trypsin/EDTA, after which they were neutralized with DMEM with 10% fetal calf serum, washed twice with PBS, and filtered through a 35-mm pore size nylon screen. FACS analysis was performed on a flow cytometer with a 488-nm argon laser and GFP-positive cells were isolated.

RT-PCR and real-time PCR

Total RNA from the cultured cells was extracted using the Trizol reagent (Invitrogen). RT-PCR was performed as described previously (18). The reaction mixture was subjected to electrophoresis in a 1.5% agarose gel, and the resulting bands were visualized by staining with ethidium bromide. Real-time PCR was performed as described by Rutledge and Cote (19). Reagents for real-time PCR were purchased from Applied Biosystems (Warrington, UK), except for SYBER green PCR master mix (QIAGEN, Valencia, CA). Reactions were carried out and fluorescence was detected on a GeneAmp 7700 system (Applied Biosystems). The primers used are shown in Table 1.

Western blot analysis

The extraction of protein from the cultured cells and subsequent quantification was performed as described previously (20). Equal amounts of protein (50 μg) were resolved by 12.5% SDS-PAGE and transferred to polyvinylidene difluoride membranes. Western blot analyses of SF-1, steroidogenic acute regulatory protein (StAR), P450scc, 3β-HSD I, P450c17, and β-tubulin were carried out with antisera directed against SF-1 (Ad4BP, kindly provided by Dr. K. Morohashi, National Institute of Basic Biology, Okazaki, Japan), StAR (kindly provided by Dr. W. Miller, University of California, San Francisco, CA) (21), P450scc (kindly provided by Dr. B. C. Chung) (22), 3β-HSD I (kindly provided by Dr. A. Payne), P450c17 (kindly provided by Dr. D. Hales) (23), and β-tubulin (D-10, Santa Cruz). ECL Western blot reagents (Amersham Pharmacia Biotech, Piscataway, NJ) were used for detection.

Results

Transplantation of rat bone marrow mesenchymal stem cells

In the prepubertal testis, fetal-type Leydig cells are replaced by adult-type Leydig cells, which originate from mesenchymal precursor cells that are present in the testicular interstitium (12). To determine whether MSCs can be engrafted into the testis and converted into steroidogenic cells we took 1×10^6 bone marrow cells from TgN(ActbEGFP) transgenic rats that had been maintained in culture (Fig. 1A) and injected them into the testes of 3-wk-old SD rats. As shown in Fig. 1C, donor engraftment was confirmed (100%) at various periods after transplantation (1–4 wk). A histochemical examination revealed that the GFP-positive cells present in the testes were located in the interstitium and were not observed within the seminiferous tubules (Fig. 1D). An immunohistochemical study showed that most of the GFP-positive cells in the interstitium were also positive for three Leydig cell markers, P450scc (Fig. 1E), 3β-HSD I, and P450c17 (data not shown). These results indicate that donor derived-plastic adhered marrow cells had in fact differentiated into steroidogenic Leydig-like cells *in vivo*.

Gene promoter sorting

Although these data suggest that the injected stem cells differentiated into Leydig cells, the apparent stem cell plasticity may also be explained by possible cell-nuclear fusion between donor and recipient cells, as has been recently suggested (24). Therefore, we next performed *in vitro* experiments to determine whether purified murine MSCs (mMSCs), KUM9 (15), have the capacity to differentiate into steroidogenic cells. To detect a cell population committed to

TABLE 1. Primers for RT-PCR and real-time PCR

Gene	Sequence	Gene	Sequence
RT-PCR		RT-PCR	
SF-1	F-CGCACAGTCCAGAACAACAAGCA R-CGGTTAGAGAAGGCAGGATAGAG	hHSD3b2	F-CAGTGTGCCAGTCTTCATCT R-AGCAGGAAGCCAATCCAGTA
mStAR	F-GAAGGAAAGCCAGCAGGAGAACG R-CTCTGATGACACCACTCTGCTCC	hP450c17	F-CATGCTGGACACACTGATGC R-GGTTGTATCTCTAAAATCTGT
mP450scc	F-TTCCGCTTTTCCTTTGAGTCCAT R-GTGTCTCCTTGATGCTGGCTTTC	hHSD17b3	F-GCAGATTTTACAAAAGATGACAT R-TCATGGGCAAGGCAGCCACAGGT
mHSD3b1	F-ACTGCAGGAGGTCAGAGCT R-GCCAGTAACACAGAATACC	hP450c21	F-TGCCTGCCTATTACAAATGT R-GGTGAAGCAAAAAAACCACG
mHSD3b6	F-TCTGGAGGAGATCAGGGTC R-GCCCGTACAACCGAGAATATT	hP45011 b1	F-ACATTGGTGCGCGTGTTCCTC R-GAGACGTGATTAGTTGATGGC
mP450c17	F-AAATAATAACACTGGGGAAGGC R-TGGGTGTGGGTGTAATGAGATGG	hP450 11b2	F-TACAGGTTTTCCTCTACTCG R-AGATGCAAGACTAGTTAATC
mP450c21	F-AGAGGATCCGCTTGGGGCTGC R-GGAGGAATTCCTTATGGATGGC	hP450aro	F-CTGGAAGAATGTATGGACTT R-GATCATTTCCAGCATGTTTT
mP450 11b1	F-TCACCAAATGTATCAAGAATGTGT R-CCATCTGCACATCCTCTTTCTCTT	β-Actin	F-GGGAAATCGTGCGTGACATTAAG R-TGTGTTGGCGTACAGGTCTTTG
mP450 11b2	F-CCAACAGATGTATCTGGAAGGTGC R-CCATCTGCACATCCTCTTGCCTCA	hIGF-2	F-AGTCGATGCTGGTGCTTCTACCTCTT R-TGCGGCAGTTTTGCTCACTTCCGATT
mLHR	F-CTCCACCTATCTCCCTGTC R-TCTTTCTTCGGCAAATTCCTG	Real-time PCR	
mACTHR	F-GCTCCAAGGATCATTTACTTGC R-CGCCAGGAGGCTTAACATAAC	mP450scc	F-CCAGTGTCCCCATGCTCAAC R-TGCATGGTCCTTCCAGGTCT
GAPDH	F-ACCACAGTCCATGCCATCAC R-TCCACCACCCTGTTGCTGA	mHSD3b1	F-TAACAATTTAACAGCCCCTCCTAAGG R-ATCCAGCCATGGTCAACACA
GFP	F-TGACCACCCTGACCTACGGCGT R-GGTAGTGGTTGTCGGGCAGCA	mHSD3b6	F-AAACCATCCTCCACTGTTCTAGCT R-TGGAGATGGTCAGCCACAAG
mHSD17b3	F-ATTTTACCAGACAAGACATCT R-GGGGTCAGCACCTGAATAATG	mP450c17	F-AGTTTGCCATCCCGAAGGA R-CTGGCTGGTCCATTCATTT
mP450aro	F-TCAATACCAGGTCCTGGCTA R-GTATGCACTGATTCACGTTC	mHSD17b3	F-TGGGACAATGGGCAGTGAT R-GCCAACTCAAATGAATAGGCTTTC
hStAR	F-GAGAGTCAGCAGGACAATGG R-CTGGTTGATGATGCTCTTGG	β-Actin	F-CAACCGTGAAAAGATGACCCAGATC R-AGTCCATCACAATGCCTGTGGTAC
hP450scc	F-TAGTGTCTCCTTGATGCTGG R-GAAAGGAAGTGTTCACCACG		

F, Forward; R, reverse.

the steroidogenic lineage, we first introduced a human CYP11A1 promoter/GFP gene construct into the mMSCs. This was accomplished by using a 2.3-kb fragment of the promoter region of the human CYP11A1 (a gene that encodes cytochrome P450scc, cholesterol side-chain cleavage enzyme), which has been shown to selectively drive transgene expression to adrenal and gonadal steroidogenic cells (17). In some of the transformed cell lines, GFP fluorescence was detected, as shown in Fig. 2, B and C, but the number of GFP-expressing cells was very low. Thus, GFP-positive cells were enriched by sorting with flow cytometry (Fig. 2E, 1–5% of total cells). As shown in Fig. 2, F and G, enriched GFP-positive cells were also positive for P450scc, indicating that a very small but distinct portion of the mMSCs had spontaneously differentiated into cells that produce the steroid hormone-synthesizing enzyme. Further analysis of the differentiated cells revealed the expression of several genes that are specific to testicular Leydig cells, as shown in Fig. 2H. These include a nuclear orphan receptor SF-1, 3β-HSD types I and VI, and LH receptor (Fig. 2H, lane SCC+). LH receptor and 3β-HSD VI are known to be typical markers for androgen producing cells, such as Leydig cells (25). These observations further support the *in vivo* findings that rodent MSCs have the capacity to differentiate into Leydig-like cells in the testis.

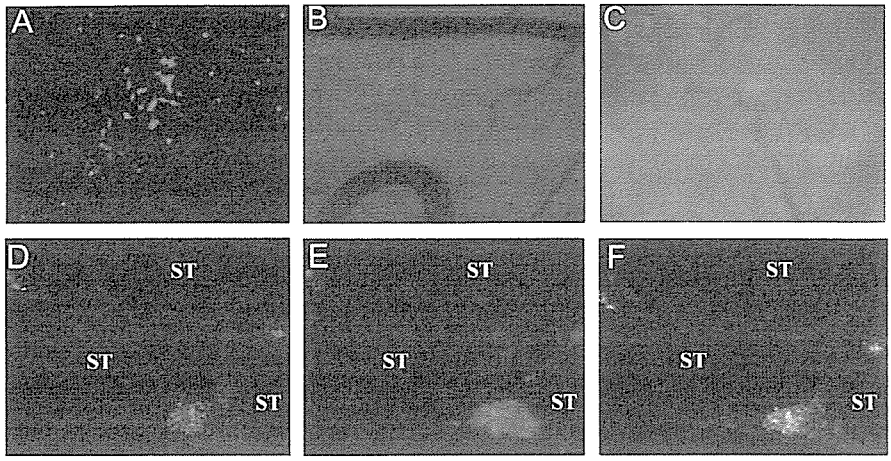

FIG. 1. Transplantation of GFP-positive MSCs into the testis. A, Fluorescence view of MSCs from a green rat 3 d after the first passage. Fluorescence microscopic view of testis before (B) or 3 wk after (C) MSC transplantation. Double staining of frozen sections from the testis 5 wk after MSC transplantation with anti-GFP (D) and anti-P450scc (E) antibodies. F, Merged fluorescent image of D and E. ST, Seminiferous tubule.

Stable transfection of SF-1 into mouse MSCs

It is noteworthy that SF-1 expression was induced in the GFP-positive cells (Fig. 2H). SF-1, also known as Ad4BP, regulates the cell-specific expression of a variety of proteins that are involved in steroidogenesis, in addition to its roles in reproduction and gonadal differentiation (26). Therefore, we next examined the effects of the stable transfection of SF-1 to mMSCs. Various cell lines that stably express SF-1 were isolated. As shown in Fig. 3C, SF-1-induced morphological changes in the cells, such as the accumulation of numerous lipid droplets. However, the transformed cells did not express steroidogenic enzyme genes or produce any steroid

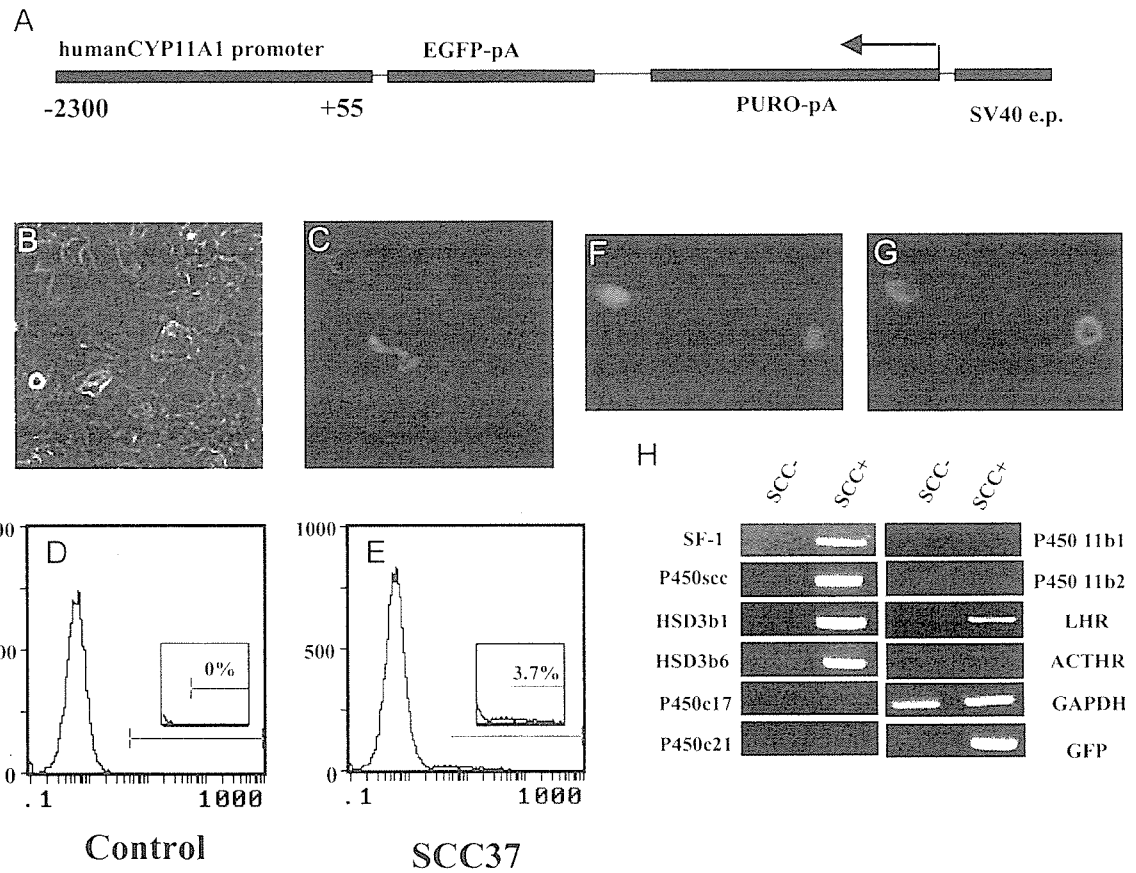

FIG. 2. Spontaneous differentiation of KUM9 into steroidogenic cells. A, Schematic representation of the SCC-reporter gene (SCC-GFP). The SCC-GFP reporter plasmid contains the 2300-bp upstream sequence of the human CYP11A1 gene and the puromycin-*N*-acetyltransferase gene (PURO-pA) driven by the Simian virus 40 early promoter (SV40 e.p.). Phase-contrast (B) and fluorescent (C) images of mMSCs transfected with SCC-GFP and selected by puromycin are shown. Flow cytometric analysis of enhanced GFP (EGFP) expression in KUM9 transfected with control-GFP (D) or SCC-GFP (E) are shown. KUM9-derived cells expressing GFP (F) under the control of the human CYP11A1 promoter were immunocytochemically stained with anti-P450scc antibody (G). H, SCC-GFP-positive (SCC+) and negative (SCC−) populations were sorted and analyzed for various marker genes by RT-PCR.

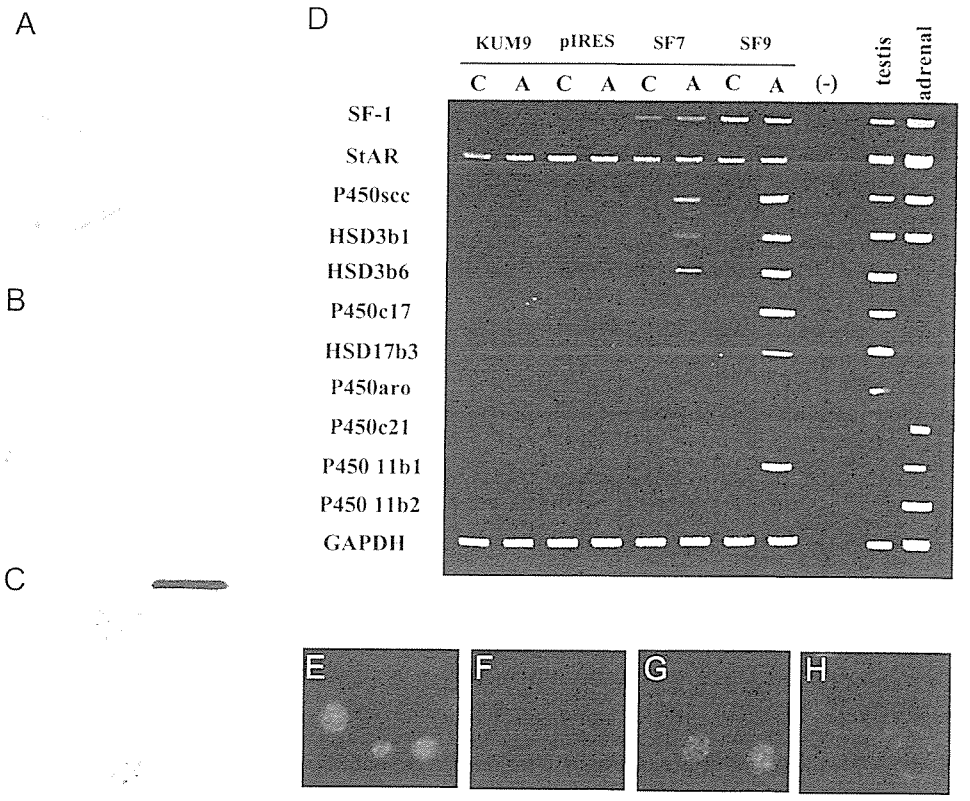

FIG. 3. Differentiation of KUM9 into steroidogenic cells. Phase-contrast images of mMSCs untransfected (A) or stably transfected with the control (B) or the SF-1-expression (C) vectors are shown. An immunoblot analysis was performed with an antibody against SF-1 (*insets*). D, RT-PCR analysis of each clones cultured with or without 8-bromoadenosine-cAMP (8br-cAMP) for 7 d (C: without 8br-cAMP; A: with 8br-cAMP). Data were compared with those from mouse adrenal and testicular tissues. Fluorescent images of 4′,6′-diamino-2-phenylindole staining (E and G) and a P450scc immunostaining (F and H) of KUM9 transfected with the SF-1-expressing vector and then cultured with (G and H) or without 8br-cAMP (E and F).

hormones (Fig. 3D and Table 2). Therefore, we next added cAMP to the cultures because cAMP is known to induce steroidogenesis in a number of steroidogenic cell lines. Treatment of confluent cultures with cAMP was found to induce both P450scc mRNA (Fig. 3D) and protein (Fig. 3H) in the transformed cell lines, SF7 and SF9, whereas no induction was observed in untransfected (KUM9) or vector-transfected (pIRES) mMSCs (Fig. 3D). Treatment of the cells for a period of 7 d further induced the expression of other steroidogenic enzyme genes, as shown in Fig. 3D. Several cell lines showed similar expression patterns (two of which are shown in Fig. 3D).

3β-HSD types I and VI were induced 3 d after cAMP treatment (Fig. 4). In the testis, the formation of testosterone is dependent on 3β-HSD activity, and isoform types I and VI have been shown to be expressed in the adult mouse testis (27). P450c17 and 17β-hydroxysteroid dehydrogenase III (17β-HSD III) were induced 5 d after the treatment (Fig. 4). It is interesting to note that the order of induction of the enzymes is similar to the sequential order for the steroid hormone synthetic pathway. 3β-HSD enzymes are essential for the production of progesterone, and P450c17 and 17β-HSD III are both required for the production of testosterone in testicular Leydig cells. Consistent with the expression pattern of the steroidogenic enzymes, testosterone was the major sex steroid hormone produced in the transformed cell line, SF9, when treated with cAMP for 7 d (Table 2). Two adrenal-specific steroid hormones, glucocorticoids and mineralocorticoids, were not detected in these cells. These results clearly demonstrate that the stable expression of SF-1 and the addition of cAMP induced the differentiation of mMSCs into steroidogenic cells and that these cells have properties that are similar to those of testicular Leydig cells.

TABLE 2. Production of steroid hormones by MSCs stably expressing SF-1 (SF9-KUM9 or SF4-hMSC) in the presence (+) or absence (−) of 8br-cAMP (ng/ml)

Cell (cAMP)	Progesterone	Testosterone	Estradiol	Glucocorticoid	Aldosterone
pIRES-KUM9 (−)	N.D.	N.D.	N.D.	N.D.	N.D.
pIRES-KUM9 (+)	N.D.	N.D.	N.D.	N.D.	N.D.
SF9-KUM9 (−)	N.D.	N.D.	N.D.	N.D.	N.D.
SF9-KUM9 (+)	24.3 ± 4.25	1.6 ± 0.29	N.D.	N.D.	N.D.
pIRES-hMSC (−)	N.D.	N.D.	N.D.	N.D.	N.D.
pIRES-hMSC (+)	N.D.	N.D.	N.D.	N.D.	N.D.
SF4-hMSC (−)	N.D.	N.D.	N.D.	N.D.	N.D.
SF4-hMSC (+)	270 ± 82.5	17.5 ± 0.20	0.21 ± 0.11	520 ± 200	1.56 ± 0.42

Data are means and SEM values of at least duplicate assays. N.D., No detectable values.

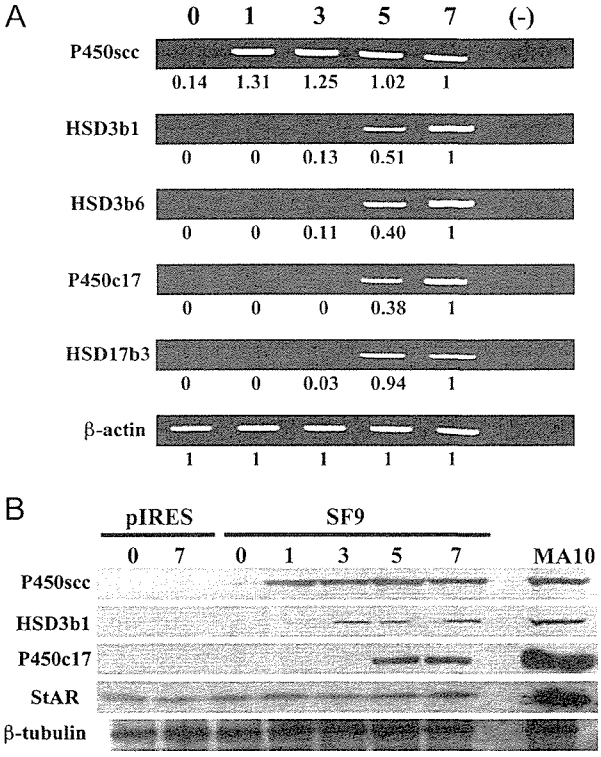

FIG. 4. Time-dependent induction of steroidogenic enzymes by cAMP. KUM9 cells stably transfected with SF-1-expression (SF9) or control (pIRES) vector were cultured and treated with 8-bromoadenosine-cAMP for the indicated times. A, P450scc, 3β-HSD I, 3β-HSD VI, P450c17, and 17β-HSD III mRNA levels were analyzed by RT-PCR and real-time PCR. Real-time PCR data are the mean values of at least triplicate assays. The 7-d value was arbitrarily taken as 1.0. B, Immunoblot analyses were performed with antibodies against StAR, P450scc, 3β-HSD I, P450c17, and β-tubulin using the same lysates. The data were compared with that from MA-10 cells treated with cAMP (4 h).

Stable transfection of SF-1 into human MSCs

We next examined the issue of whether the same approach could also be used to induce the differentiation of human MSCs (hMSCs) into steroidogenic cells. Similar to the results obtained with mMSCs, hMSCs (hMSC-TERT-E6/E7) expressed no steroidogenic enzymes or StAR before transfection with SF-1 even after cAMP treatment (Fig. 5). After SF-1 transfection, all the transformed cell lines became positive for StAR gene expression, and the expression levels were further increased by cAMP treatment. Most of the steroidogenic enzymes, P450scc, 3β-HSD II, P450c17, cytochrome P450 steroid 21-hydroxylase (P450c21), cytochrome P450 aromatase (P450arom), and cytochrome P450 steroid 11 β-hydroxylase, were also substantially induced by cAMP stimulation. A significant difference between mMSCs and hMSCs was the strong expression of the P450c21 gene in the case of hMSCs. This caused a difference in the kinds of steroids produced by mMSCs and hMSCs. As listed in Table 2, glucocorticoids were the major steroids produced by the transformed hMSCs, hSF4, whereas testosterone was the major product from the transformed mMSCs, mSF9. The hSF4 cells mainly produced cortisol, the major glucocorticoid produced by the human adrenal gland. These results clearly demonstrate that the stable expression of SF-1 and subsequent cAMP treatment induced the differentiation of hMSCs into steroidogenic cells. In addition, the cortisol-producing cells also expressed ACTH receptors and can respond to ACTH for the quick production of cortisol at nanomolar levels (data not shown).

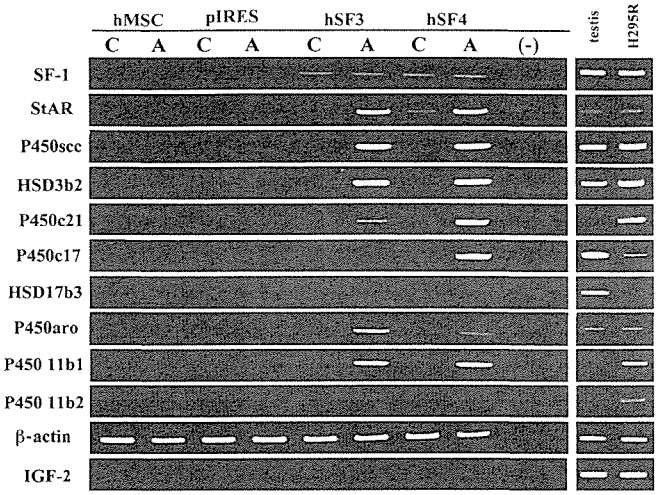

FIG. 5. Induction of steroidogenic enzymes in hMSCs. hMSCs were stably transfected with the control (pIRES) or SF-1-expression (SF3, -4) vector. RT-PCR analysis of each clone was cultured with or without 8-bromoadenosine-cAMP (8br-cAMP) for 7 d (C: without 8br-cAMP; A: with 8br-cAMP). The data were compared with that from human testis and NCI-H295R, a human adrenocortical tumor cell line, treated with cAMP (24 h).

Human MSCs also expressed P450arom as in the case of the human adrenocortical carcinoma NCI-H295R cell line (Fig. 5), whereas normal adrenal cells do not express it (28). However, hSF3 or -4 did not express IGF-II, an adrenocortical tumor marker. It has recently been shown that P450arom is expressed in human bone marrow stroma cells under certain conditions (29). Thus, it is probable that the expression of P450arom in hMSCs was not the result of a malignant phenotype or the differentiation of the cells by SF-1 and cAMP treatment.

Stable transfection of SF-1 into cells other than MSCs

We next examined the effects of transfection of SF-1 into several cell lines other than MSCs, *i.e.* a human cell line HEK293, murine embryonic stem cells, and murine cell lines F9 and NIH3T3. None of the transfected cell lines autonomously produced steroid hormones, although some were induced to express the P450scc and 3β-HSD genes (Fig. 6).

Discussion

The findings presented herein demonstrate that rodent MSCs have the potential to differentiate into steroidogenic cells with characteristics that are very similar to testicular Leydig cells. It has been postulated that mesenchymal progenitors of Leydig cells are present in the testicular interstitium (12). Immature Leydig cells are gradually replaced by mature Leydig cells that are thought to differentiate from these mesenchymal progenitors during the prepubertal period. In fact, the injection of MSCs into the testis during this critical period caused the differentiation of MSCs into steroidogenic cells that were indistinguishable from Leydig cells. Concerning the *in vivo* experiments, the possibility of

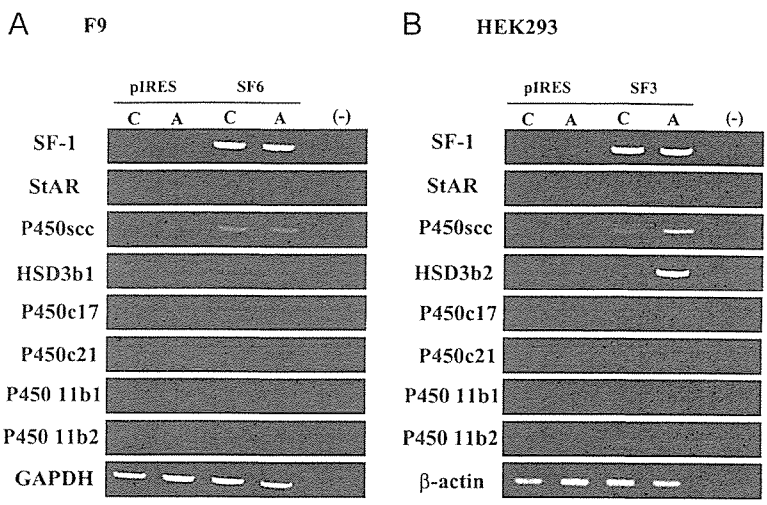

FIG. 6. Stable transfection of SF-1 and cAMP treatment for F9 (A) and HEK293 cells (B). RT-PCR analysis of steroidogenesis-related genes in each stable cell line transfected with SF-1 or pIRES (control) cultured with or without 8-bromoadenosine-cAMP (8br-cAMP) for 7 d (C: without 8br-cAMP; A: with 8br-cAMP).

cell fusion between donor MSCs and recipient testicular Leydig cells or their progenitor cells cannot be excluded. However, it should be emphasized that very small but distinct portions of mMSCs underwent spontaneous differentiation into Leydig-like cells *in vitro*. Lo *et al.* (30) demonstrated, by means of a cell transplantation assay, the presence of stem cells or progenitors for Leydig cells. Therefore, our data strongly suggest that bone marrow-derived MSCs share common properties with testicular MSCs or Leydig cell progenitors. Conversely, testicular MSCs or Leydig cell progenitors might also have pluripotent characteristics, similar to bone marrow-derived MSCs, as has been reported for some other MSCs (4, 31).

In addition, transfection of cultured mMSCs with SF-1 followed by cAMP stimulation resulted in their differentiation into Leydig cells. The same procedure also led to the successful induction of hMSCs into steroidogenic cells. In this case, however, most of the cell lines expressing SF-1 largely produced glucocorticoids rather than testosterone. This was mainly due to the strong induction of P450c21 gene expression in the hMSCs. To investigate the issue of whether hMSCs are able to differentiate into Leydig cells, we also injected hMSCs to the testis of nude mice or rats (data not shown). Unfortunately, the human cells did not survive for more than several weeks in the rodent testis.

Because the established cell lines need much longer times than general steroidogenic cells to produce steroid hormones by cAMP stimulation in this study, we speculate that cAMP treatment of this study is necessary for the induction of the cellular differentiation rather than direct stimulation of gene transcription of steroidogenic enzymes.

In hMSCs, the stable expression of SF-1 and cAMP treatment induced the expression of the StAR gene, which is essential for the transfer of cholesterol from the outer to the inner membrane of mitochondria in which the conversion of cholesterol to steroid hormones begins (21). The same treatment failed to induce StAR gene expression in several cell lines (other than MSCs) including embryonic stem (ES) cells and therefore failed to induce any steroid hormones. The expression of the P450scc or 3β-HSD gene was induced at low levels in some of them, however (Fig. 6). It has been reported that the stable transfection of SF-1 into ES cells results in morphological changes and the induction of P450scc enzyme expression, (32). No autonomous production of steroid hormones was observed, however, probably because of the deficiency of cholesterol storage and mobilization and the lack of StAR protein expression (32). Therefore, our present observations suggest that MSCs, but not ES cells, are excellent precursors of steroidogenic cells. In contrast to human cells, StAR was constitutively expressed in KUM9 as well as the freshly isolated rat MSCs (our unpublished data). Therefore, we speculate that StAR gene expression is not always under the control of SF-1, and the pattern of expression may be different between species, even in the same tissues. In addition to the steroidogenesis, the movement of cholesterol to the inner mitochondrial membrane is also important for its metabolism, because one of the rate-determining steps, the 27-hydroxylation of cholesterol, is catalyzed by sterol 27-hydroxylase, which is located in the inner mitochondrial membrane (33, 34). Cholesterol metabolites, such as oxysterols have been proposed to be potential regulators of genes in cholesterol homeostasis (33). We found that sterol 27-hydroxylase mRNA was detectable in rat and mouse MSCs (data not shown), suggesting that it is involved in cholesterol metabolism. Therefore, it is assumed that the StAR protein in KUM9 is present to promote the cholesterol metabolism, despite the fact that steroidogenesis does not take place. In support of this hypothesis, ectopic expression of the StAR protein increases the metabolism of cholesterol in rat primary hepatocytes (34).

Gondo *et al.* (35) recently reported that the adenovirus-mediated forced expression of SF-1 transforms primary long-term cultured murine bone marrow cells into ACTH-responsive steroidogenic cells. In contrast to our observation obtained from murine MSCs, their steroidogenic cells produce both gonadal and adrenal steroids. There are two possible explanations for their results: 1) their cells were a mixed adrenal/gonadal phenotype or 2) were a mixture of adrenal or gonadal phenotypic cells. The latter seems to be more likely because our study clearly demonstrated the differentiation of adult stem cells derived from both murine and human into gonadal or adrenal steroidogenic cells. Therefore, with respect to the difference between mouse and human cells, we assume that the mouse MSCs used in our study were already committed to the gonadal lineage, whereas the hMSCs were already committed to

the adrenal lineage. In support of this hypothesis, it has frequently been reported that MSCs are heterogeneous populations that have a different differentiation potential (1, 2, 10). In a future study, the same treatment of various mouse or human MSCs need to be carried out, followed by observations of whether both adrenal and gonadal phenotypes are obtained. This might also provide a tool for revealing the pathway leading to the differentiation of the cells into adrenal or gonadal steroidogenic cells.

In summary, we demonstrate here that MSCs have the capacity to differentiate into steroidogenic cells, both *in vivo* and *in vitro*. MSCs represent not only a powerful tool for studies of the differentiation of the steroidogenic lineage but may also offer a possible clinical stem cell resource for diseases of steroidogenic organs.

Acknowledgments

We are grateful to Drs. K. Morohashi, W. Miller, B. C. Chung, A. Payne, and D. Hales for providing plasmids and antisera. We also thank Drs. M. Ascoli and J. Toguchida for the generous gifts of MA10 and hMSCs and Ms. Y. Inoue, T. Satake, and K. Matsuura for technical assistance.

Received February 8, 2006. Accepted May 16, 2006.

Address all correspondence and requests for reprints to: Kaoru Miyamoto, Department of Biochemistry, Faculty of Medical Sciences, University of Fukui, Shimoaizuki, Matsuoka-cho, Fukui 910-1193, Japan. E-mail: kmiyamot@fmsrsa.fukui-med.ac.jp.

This work was supported in part by a grant from the Smoking Research Foundation and the 21st Century Center of Excellence Program (Medical Science).

All authors (T.Y., T.M., K.Y., H.K., T.S., M.Y., T.K., Z.S., A.U., K.M.) have nothing to declare.

References

1. **Friedenstein AJ, Gorskaja JF, Kulagina NN** 1976 Fibroblast precursors in normal and irradiated mouse hematopoietic organs. Exp Hematol 4:267–274
2. **Prockop DJ** 1997 Marrow stromal cells as stem cells for nonhematopoietic tissues. Science 276:71–74
3. **Ferrari G, Cusella-De Angelis G, Coletta M, Paolucci E, Stornaiuolo A, Cossu G, Mavilio F** 1998 Muscle regeneration by bone marrow-derived myogenic progenitors. Science 279:1528–1530
4. **Lee OK, Kuo TK, Chen WM, Lee KD, Hsieh SL, Chen TH** 2004 Isolation of multipotent mesenchymal stem cells from umbilical cord blood. Blood 103: 1669–1675
5. **D'Amour KA, Gage FH** 2003 Genetic and functional differences between multipotent neural and pluripotent embryonic stem cells. Proc Natl Acad Sci USA 100(Suppl 1):11866–11872
6. **De Ugarte DA, Morizono K, Elbarbary A, Alfonso Z, Zuk PA, Zhu M, Dragoo JL, Ashjian P, Thomas B, Benhaim P, Chen I, Fraser J, Hedrick MH** 2003 Comparison of multi-lineage cells from human adipose tissue and bone marrow. Cells Tissues Organs 174:101–109
7. **Kopen GC, Prockop DJ, Phinney DG** 1999 Marrow stromal cells migrate throughout forebrain and cerebellum, and they differentiate into astrocytes after injection into neonatal mouse brains. Proc Natl Acad Sci USA 96:10711–10716
8. **Ortiz LA, Gambelli F, McBride C, Gaupp D, Baddoo M, Kaminski N, Phinney DG** 2003 Mesenchymal stem cell engraftment in lung is enhanced in response to bleomycin exposure and ameliorates its fibrotic effects. Proc Natl Acad Sci USA 100:8407–8411
9. **Chamberlain JR, Schwarze U, Wang PR, Hirata RK, Hankenson KD, Pace JM, Underwood RA, Song KM, Sussman M, Byers PH, Russell DW** 2004 Gene targeting in stem cells from individuals with osteogenesis imperfecta. Science 303:1198–1201
10. **Prockop DJ, Gregory CA, Spees JL** 2003 One strategy for cell and gene therapy: harnessing the power of adult stem cells to repair tissues. Proc Natl Acad Sci USA 100(Suppl 1):11917–11923
11. **Hatano O, Takakusu A, Nomura M, Morohashi K** 1996 Identical origin of adrenal cortex and gonad revealed by expression profiles of Ad4BP/SF-1. Genes Cells 1:663–671
12. **Roosen-Runge EC, Anderson D** 1959 The development of the interstitial cells in the testis of the albino rat. Acta Anat (Basel) 37:125–137
13. **Holmes PV, Dickson AD** 1971 X-zone degeneration in the adrenal glands of adult and immature female mice. J Anat 108:159–168
14. **Pochampally RR, Neville BT, Schwarz EJ, Li MM, Prockop DJ** 2004 Rat adult stem cells (marrow stromal cells) engraft and differentiate in chick embryos without evidence of cell fusion. Proc Natl Acad Sci USA 101:9282–9285
15. **Makino S, Fukuda K, Miyoshi S, Konishi F, Kodama H, Pan J, Sano M, Takahashi T, Hori S, Abe H, Hata J, Umezawa A, Ogawa S** 1999 Cardiomyocytes can be generated from marrow stromal cells in vitro. J Clin Invest 103:697–705
16. **Okamoto T, Aoyama T, Nakayama T, Nakamata T, Hosaka T, Nishijo K, Nakamura T, Kiyono T, Toguchida J** 2002 Clonal heterogeneity in differentiation potential of immortalized human mesenchymal stem cells. Biochem Biophys Res Commun 295:354–361
17. **Hu MC, Chou SJ, Huang YY, Hsu NC, Li H, Chung BC** 1999 Tissue-specific, hormonal, and developmental regulation of SCC-LacZ expression in transgenic mice leads to adrenocortical zone characterization. Endocrinology 140: 5609–5618
18. **Mizutani T, Yamada K, Yazawa T, Okada T, Minegishi T, Miyamoto K** 2001 Cloning and characterization of gonadotropin-inducible ovarian transcription factors (GIOT1 and -2) that are novel members of the (Cys)(2)-(His)(2)-type zinc finger protein family. Mol Endocrinol 15:1693–1705
19. **Rutledge RG, Cote C** 2003 Mathematics of quantitative kinetic PCR and the application of standard curves. Nucleic Acids Res 31:e93
20. **Yazawa T, Mizutani T, Yamada K, Kawata H, Sekiguchi T, Yoshino M, Kajitani T, Shou Z, Miyamoto K** 2003 Involvement of cyclic adenosine 5′-monophosphate response element-binding protein, steroidogenic factor 1, and Dax-1 in the regulation of gonadotropin-inducible ovarian transcription factor 1 gene expression by follicle-stimulating hormone in ovarian granulosa cells. Endocrinology 144:1920–1930
21. **Bose HS, Whittal RM, Baldwin MA, Miller WL** 1999 The active form of the steroidogenic acute regulatory protein, StAR, appears to be a molten globule. Proc Natl Acad Sci USA 96:7250–7255
22. **Hu MC, Guo IC, Lin JH, Chung BC** 1991 Regulated expression of cytochrome P-450scc (cholesterol-side-chain cleavage enzyme) in cultured cell lines detected by antibody against bacterially expressed human protein. Biochem J 274(Pt 3):813–817
23. **Hales DB, Sha LL, Payne AH** 1987 Testosterone inhibits cAMP-induced *de novo* synthesis of Leydig cell cytochrome P-450(17α) by an androgen receptor-mediated mechanism. J Biol Chem 262:11200–11206
24. **Medvinsky A, Smith A** 2003 Stem cells: fusion brings down barriers. Nature 422:823–825
25. **O'Shaughnessy PJ, Willerton L, Baker PJ** 2002 Changes in Leydig cell gene expression during development in the mouse. Biol Reprod 66:966–975
26. **Parker KL, Schimmer BP** 1997 Steroidogenic factor 1: a key determinant of endocrine development and function. Endocr Rev 18:361–377
27. **Peng L, Arensburg J, Orly J, Payne AH** 2002 The murine 3β-hydroxysteroid dehydrogenase (3β-HSD) gene family: a postulated role for 3β-HSD VI during early pregnancy. Mol Cell Endocrinol 187:213–221
28. **Staels B, Hum DW, Miller WL** 1993 Regulation of steroidogenesis in NCI-H295 cells: a cellular model of the human fetal adrenal. Mol Endocrinol 7:423–433
29. **Heim M, Frank O, Kampmann G, Sochocky N, Pennimpede T, Fuchs P, Hunziker W, Weber P, Martin I, Bendik I** 2004 The phytoestrogen genistein enhances osteogenesis and represses adipogenic differentiation of human primary bone marrow stromal cells. Endocrinology 145:848–859
30. **Lo KC, Lei Z, Rao Ch V, Beck J, Lamb DJ** 2004 *De novo* testosterone production in luteinizing hormone receptor knockout mice after transplantation of Leydig stem cells. Endocrinology 145:4011–4015
31. **De Bari C, Dell'Accio F, Tylzanowski P, Luyten FP** 2001 Multipotent mesenchymal stem cells from adult human synovial membrane. Arthritis Rheum 44:1928–1942
32. **Crawford PA, Sadovsky Y, Milbrandt J** 1997 Nuclear receptor steroidogenic factor 1 directs embryonic stem cells toward the steroidogenic lineage. Mol Cell Biol 17:3997–4006
33. **Bjorkhem I** 2002 Do oxysterols control cholesterol homeostasis? J Clin Invest 110:725–730
34. **Pandak WM, Ren S, Marques D, Hall E, Redford K, Mallonee D, Bohdan P, Heuman D, Gil G, Hylemon P** 2002 Transport of cholesterol into mitochondria is rate-limiting for bile acid synthesis via the alternative pathway in primary rat hepatocytes. J Biol Chem 277:48158–48164
35. **Gondo S, Yanase T, Okabe T, Tanaka T, Morinaga H, Nomura M, Goto K, Nawata H** 2004 SF-1/Ad4BP transforms primary long-term cultured bone marrow cells into ACTH-responsive steroidogenic cells. Genes Cells 9:1239–1247

Endocrinology is published monthly by The Endocrine Society (http://www.endo-society.org), the foremost professional society serving the endocrine community.

ELSEVIER

International Journal of Cardiology xx (2006) xxx–xxx

International Journal of Cardiology

www.elsevier.com/locate/ijcard

Circulating endothelial progenitor cells in congestive heart failure ☆

Mutsuko Nonaka-Sarukawa [a], Keiji Yamamoto [a,*], Hirotaka Aoki [a], Yoshioki Nishimura [a], Hidenori Tomizawa [a], Masaru Ichida [a], Takayuki Eizawa [a], Kazuo Muroi [b], Uichi Ikeda [c], Kazuyuki Shimada [a]

[a] *Division of Cardiovascular Medicine, Jichi Medical University, Shimotsuke, Tochigi 329-0498, Japan*
[b] *Division of Cell Transplantation and Transfusion, Jichi Medical University, Shimotsuke, Tochigi 329-0498, Japan*
[c] *Department of Organ Regeneration, Shinshu University Graduate School of Medicine, Matsumoto, Nagano 390-8621, Japan*

Received 9 June 2006; accepted 29 July 2006

Abstract

Background: Endothelial progenitor cells (EPCs) circulate in the adult peripheral blood and contribute to neovascularization. EPCs are considered to be included in CD34 positive mononuclear cells ($CD34^+$ MNCs). Kinetics of circulating EPCs in congestive heart failure (CHF) has not been fully investigated.
Methods: We determined the numbers of white blood cells (WBCs), plasma brain natriuretic peptide (BNP), serum erythropoietin, vascular endothelial growth factor (VEGF) and thrombomodulin levels in 16 mild CHF patients (NYHA I, II), 10 severe CHF patients with acute exacerbation (NYHA III, IV), and 22 control subjects. The number of $CD34^+$ MNCs in peripheral blood was quantified by flow cytometry.
Results: The ratio of $CD34^+$ MNCs:10^3 WBCs in mild CHF patients was higher than that in control subjects ($P<0.05$). Interestingly, the ratio of $CD34^+$ MNCs:10^3 WBCs in severe CHF patients at admission was significantly lower than that in control subjects ($P<0.005$) or in mild CHF patients ($P<0.05$). Levels of BNP and erythropoietin in severe CHF patients were significantly higher than those in mild CHF patients. However, VEGF and thrombomodulin levels were not different between mild and severe CHF patients. In addition, the ratio of $CD34^+$ MNCs:10^3 WBCs in severe CHF patients increased in proportion to the amelioration of CHF during hospitalization, and this increase correlated with the decrease in BNP level.
Conclusions: The ratio of $CD34^+$ MNCs:10^3 WBCs was decreased in severe CHF. These findings suggest that impaired EPC recruitment might be involved in the pathophysiology of severe CHF.

Keywords: Heart failure; Endothelial progenitor cells; Brain natriuretic peptide

1. Introduction

The bone marrow-derived endothelial progenitor cells (EPCs) are considered to originate from hematopoietic stem cells, which are positive for CD34 [1,2]. Circulating EPCs home to sites of neovascularization and differentiate into endothelial cells in site [3,4] in a manner consistent with a process termed vasculogenesis [5]. EPCs and $CD34^+$ cells increase in patients with endothelial damage [6], vascular trauma [7], and acute myocardial infarction [8], which reflects increased endothelial cell turnover. Local or systemic administration of cultured or fresh EPCs enhances ischemic neovascularization and improves function of ischemic tissues in animals with hindlimb or myocardial ischemia [9,10]. Recently, the therapeutic benefits of EPC therapy were demonstrated in patients with severe ischemia in the lower limb and with acute myocardial infarction [11,12].

Despite recent therapeutic advances, congestive heart failure (CHF) leading to high mortality is a major health problem [13]. During progression to overt heart failure,

☆ This study was supported in part by a grant from the Ministry of Education, Culture, Sports, Science, and Technology of Japan (15590769), Tokyo, Japan.
* Corresponding author. Tel.: +81 285 58 7344; fax: +81 285 44 5317.
E-mail address: kyamamoto@jichi.ac.jp (K. Yamamoto).

0167-5273/$ - see front matter © 2006 Elsevier Ireland Ltd. All rights reserved.
doi:10.1016/j.ijcard.2006.07.191

Please cite this article as: Mutsuko Nonaka-Sarukawa et al., Circulating endothelial progenitor cells in congestive heart failure ☆, International Journal of Cardiology (2006), doi:10.1016/j.ijcard.2006.07.191

Table 1
Characteristics of patients with CHF

	Control	NYHA I or II	NYHA III or IV
Male/female (*n*)	16/6	8/8	6/4
Age (yrs)	52±11	57±12	68±10
NYHA functional class (n)			
I/II		7/9	
III/IV			3/7
LVEF (%)		48±18	34±15
Underlying heart disease (*n*)			
Idiopathic dilated cardiomyopathy		4	3
Valvular heart disease		5	2
Healed myocardial infarction		0	2
Hypertensive heart disease		1	1
Arrhythmia		3	2
Others		3	0
Smoking (*n*)		3	5
Diabetes mellitus (*n*)		2	4
Hypercholesterolemia (*n*)		3	2
Drugs (*n*)			
Nitrate		2	2
Calcium antagonist		3	2
Beta-blocker		6	0
ACE inhibitor		11	2
Digoxin		6	2
Diuretic		12	6

Values are mean±SEM or number of patients. ACE, angiotensin-converting enzyme; CHF, congestive heart failure; LVEF, left ventricular ejection fraction; NYHA, New York Heart Association.

reduced cardiac output and concomitant neuroendocrine activation affect the functions of several organs. Patients with heart failure show endothelial dysfunction. In heart failure, nitric oxide production is diminished, whereas rate of endothelial apoptosis is increased [14]. Recently, a mobilization of EPCs into circulation from bone marrow has been reported in patients with acute myocardial infarction and acute coronary syndrome [8]. However, little is known about the kinetics of EPC mobilization in patients with CHF, especially the course of EPC mobilization in severe CHF.

In the present study, we measured the number of $CD34^+$ mononuclear cells (MNCs), plasma brain natriuretic peptide (BNP), serum erythropoietin, vascular endothelial growth factor (VEGF) and thrombomodulin, a marker of endothelial damage, levels to elucidate the kinetics of EPC mobilization in patients with CHF.

2. Methods

2.1. Study patients

We studied 16 mild CHF outpatients with New York Heart Association (NYHA) functional class I or II (8 men and 8 women, mean age 57±12 years) and 10 severe CHF patients with NYHA functional class III or IV (6 men and 4 women, mean age 68±10 years) admitted to our hospital for acute exacerbation of CHF (Table 1). The diagnosis of heart failure was confirmed in all patients by clinical findings and noninvasive assessment of cardiac function. Left ventricular ejection fraction was determined by echocardiographic evaluation [15]. Patients with coronary artery disease were excluded by angiographic findings and/or clinical history. Patients with renal failure, infection, chronic inflammatory disease and malignancy were excluded from this study. The control group consisted of 22 healthy volunteers (16 men and 6 women, mean age 52±11 years) without cardiovascular disease. This study was approved by our institutional human investigations committee, and written informed consent was obtained from all patients and volunteers before participation.

2.2. Blood collection

In severe CHF patients with acute exacerbation of CHF, sampling was performed at admission (on day 1), and on 14 days after admission. Blood sampling was performed after a 12-hour fast. All the subjects were supine, and a 21-gauge needle was inserted into a large antecubital vein. A 5-ml sample of whole blood for plasma separation was drawn into a plastic tube containing 7.5 mg Na_2-ethylenediaminetetraacetic acid. Plasma and serum were separated by prompt centrifugation of the blood samples at 3000 ×*g* at 4 °C for 10 min. The samples were immediately frozen, and stored at −80 °C.

2.3. Flow cytometry analysis

The number of $CD34^+$ MNCs in the peripheral blood was quantified using flow cytometry (Cytron; Ortho Diagnostic Systems) [16]. In brief, white blood cells (WBCs) were dually stained with fluorescent isothiocyanate (FITC)-conjugated CD45 (Becton Dickinson Immunocytometry Systems) and phycoerythrin (PE)-conjugated CD34 (Becton). Progenitors were separated by CD45 expression and right-angle light scatter properties. Cells expressing CD34 were measured with gating on the progenitor population. For negative

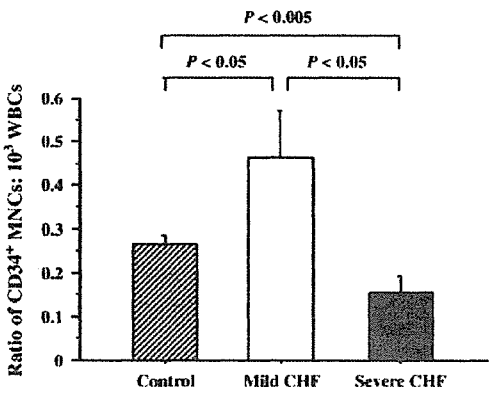

Fig. 1. The number of circulating $CD34^+$ MNCs in CHF patients. The $CD34^+$ MNC counts in control subjects (n=22), mild CHF patients with New York Heart Association (NYHA) functional class I or II (n=16) and severe CHF patients with NYHA functional class III or IV (n=10) were determined by two-color flow cytometry. Results are shown as means± SEM.

Please cite this article as: Mutsuko Nonaka-Sarukawa et al., Circulating endothelial progenitor cells in congestive heart failure ☆, International Journal of Cardiology (2006), doi:10.1016/j.ijcard.2006.07.191

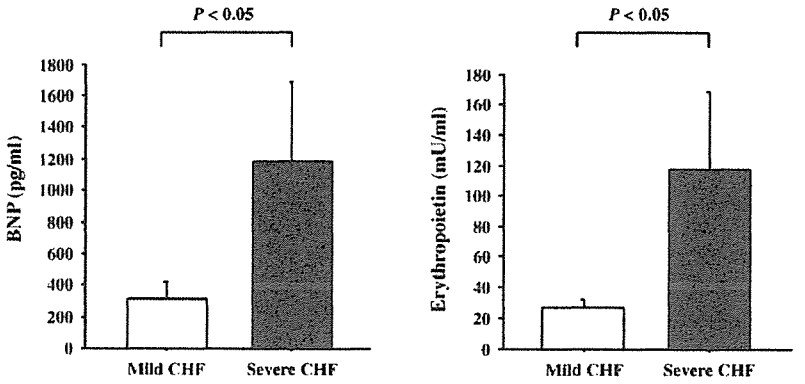

Fig. 2. Plasma BNP and serum erythropoietin levels in CHF patients. Results are shown as means±SEM.

controls, cells were stained with FITC-conjugated CD45 and PE-conjugated mouse IgG1 (Becton).

2.4. Measurements of BNP, erythropoietin, VEGF and thrombomodulin

The levels of plasma BNP and serum erythropoietin were determined by radioimmunoassay (SRL Inc., Tokyo, Japan), respectively. The sensitivity of the assays for BNP and erythropoietin was 2.0 pg/ml and 5.0 mU/ml, respectively. The levels of serum VEGF were measured using a specific enzyme-linked immunosorbent assay kit (R&D Systems) as reported previously [17]. The sensitivity of the assays for serum VEGF was 9 pg/ml. The serum levels of thrombomodulin were determined using the one-step sandwich enzyme immunoassay kit (Fuji Chemical Industries Ltd., Takaoka, Japan). The sensitivity of the assays for thrombomodulin was 1.1 FU/ml.

2.5. Statistical analysis

Data are expressed as mean±SEM. The data were analyzed by nonparametric methods to avoid assumptions about the distribution of the measured variables. ANOVA was performed with the Kruskal–Wallis method. Subsequent pairwise comparisons were made with the Mann–Whitney *U* test. The differences between baseline and posttreatment values were analyzed with the Wilcoxon signed rank test. Moreover, the association of $CD34^+$ MNCs:10^3 WBCs with other biochemical parameters was assessed by the Spearman rank correlation test. A *P*-value of <0.05 was considered significant.

3. Results

3.1. Circulating $CD34^+$ MNCs

As illustrated in Fig. 1, the ratio of $CD34^+$ MNCs:10^3 WBCs in mild CHF patients (0.46±0.11) was significantly higher than that in control subjects (0.27±0.02, $P<0.05$). Interestingly, the ratio of $CD34^+$ MNCs:10^3 WBCs in severe CHF patients at admission (0.16±0.04) was significantly lower than that in control subjects ($P<0.005$) or in mild CHF patients ($P<0.05$).

3.2. Levels of BNP, erythropoietin, VEGF and thrombomodulin in CHF

As previously reported, level of BNP, a marker of morbidity and prognostic indicators in CHF [18,19], in severe CHF patients (1183±505 pg/ml) was significantly higher

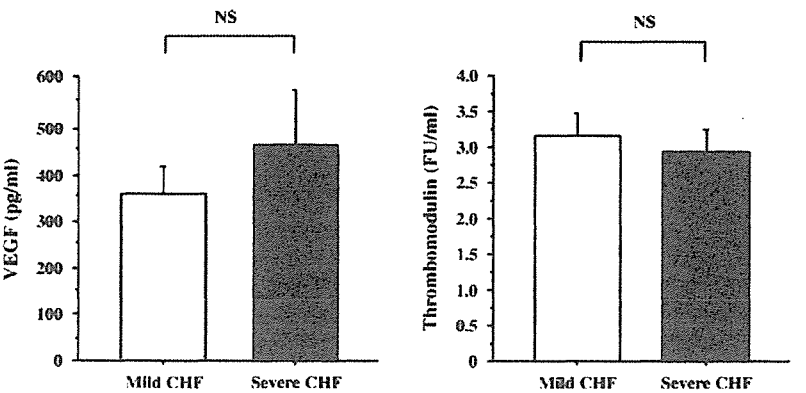

Fig. 3. Serum VEGF and thrombomodulin levels in CHF patients. Results are shown as means±SEM.

Please cite this article as: Mutsuko Nonaka-Sarukawa et al., Circulating endothelial progenitor cells in congestive heart failure ☆, International Journal of Cardiology (2006), doi:10.1016/j.ijcard.2006.07.191

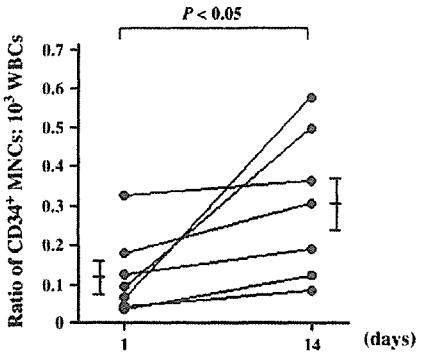

Fig. 4. The number of circulating $CD34^+$ MNCs during hospitalization in severe CHF patients. The $CD34^+$ MNC counts were determined by two-color flow cytometry. The data on day 1 represent the number of circulating $CD34^+$ MNCs in the severe CHF patients ($n=7$) at admission. Results are shown as means±SEM.

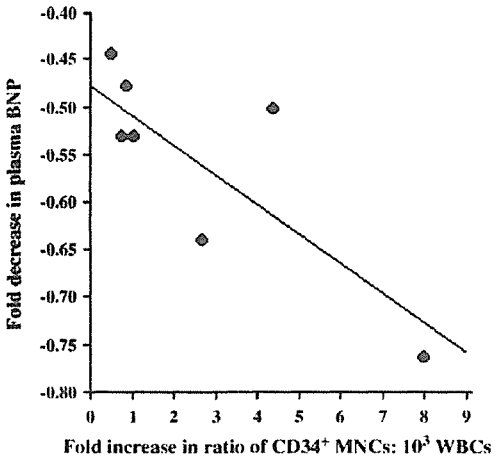

Fig. 6. Relation between increase in circulating $CD34^+$ MNCs and decrease in level of BNP. There was a high relation between increase in circulating $CD34^+$ MNCs and decrease in level of BNP during hospitalization in severe CHF ($y=-0.031x-0.48$, $r=-0.79$, $P=0.06$, $n=7$).

than that in mild CHF patients (306±117, $P<0.05$, Fig. 2). Next, we measured levels of erythropoietin and VEGF, physiologic stimuli for EPC mobilization [20,21], in CHF. Level of erythropoietin (117±52 mU/ml) in severe CHF patients was significantly higher than that (27±5, $P<0.05$) in mild CHF patients (Fig. 2). In contrast, serum VEGF level was not different between mild and severe CHF patients (355± 58 pg/ml vs. 456±116, $P=0.40$, Fig. 3). Level of thrombomodulin, a marker of endothelial damage, was not different between mild and severe CHF patients (3.2±0.3 FU/ml vs. 3.0± 0.3, $P=0.66$, Fig. 3).

3.3. Circulating $CD34^+$ MNCs and levels of BNP and erythropoietin during hospitalization in severe CHF

As shown in Fig. 4, the ratio of $CD34^+$ MNCs:10^3 WBCs in severe CHF patients (0.12±0.04) significantly increased in proportion to the amelioration of CHF during hospitalization (0.30±0.07 on 14 days after admission, $P<0.05$). In contrast, levels of BNP and erythropoietin (BNP, 1494±700 pg/ml; erythropoietin, 79±22 mU/ml) decreased in proportion to the amelioration of CHF during hospitalization (BNP, 529±162; erythropoietin, 24±6 on 14 days after admission, Fig. 5). This increase in ratio of $CD34^+$ MNCs:10^3 WBCs during hospitalization in severe CHF patients correlated with the decrease in BNP level ($y=-0.031x-0.48$, $r=-0.79$, $P=0.06$, Fig. 6).

4. Discussion

In the present study, we investigated the kinetics of circulating EPCs in CHF. We found that the number of EPCs, as measured by the number of cells expressing CD34 was significantly reduced in severe CHF patients with acute exacerbation and increased in proportion to the amelioration of CHF during hospitalization. These findings suggest that impaired EPC recruitment might be involved in the pathophysiology of severe CHF.

The mechanisms by which the condition of CHF modulates $CD34^+$ cell numbers remain to be determined. In this study, the number of $CD34^+$ MNCs significantly increased in mild CHF patients and was significantly reduced in severe

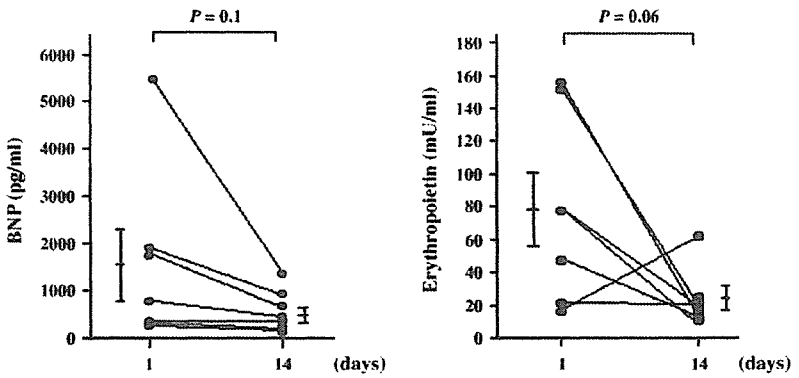

Fig. 5. Plasma BNP and serum erythropoietin levels during hospitalization in severe CHF patients. The data on day 1 represent the BNP and erythropoietin levels in the severe CHF patients at admission. Results are shown as means±SEM.

Please cite this article as: Mutsuko Nonaka-Sarukawa et al., Circulating endothelial progenitor cells in congestive heart failure ☆, International Journal of Cardiology (2006), doi:10.1016/j.ijcard.2006.07.191

CHF patients with acute exacerbation. Injury to the heart causes hematopoietic progenitor cells to migrate to the site of damage and to undergo progenitor cell differentiation [22,23]. This mechanism may contribute to the increase in $CD34^+$ MNCs observed in mild CHF patients. Iversen et al. [24] found decreased hematopoiesis in bone marrow of mice with CHF. In severe CHF, suppressed bone marrow function may lead to decrease in $CD34^+$ MNCs. An exhaustion of progenitor cells in the advanced phases of the disease could contribute to the biphasic bone marrow pattern of response to heart failure.

Increasing evidence suggests several growth factors and cytokines formerly thought to be specific for the hematopoietic system. Serum levels of erythropoietin and VEGF are associated with the number of stem and progenitor cells in the bone marrow as well as the number and function of circulating EPCs [21]. In this study, we investigated levels of erythropoietin and VEGF, two potent physiologic stimuli for EPC mobilization. Level of erythropoietin in severe CHF patients was significantly higher than that in mild CHF patients, but not serum VEGF level. These findings suggest that bone marrow suppression in severe CHF secondarily may induce the increase in erythropoietin level. In addition, the levels of serum thrombomodulin were not different between mild and severe CHF patients. These observations suggest that endothelial damage in CHF is unlikely related to the modulation of circulating $CD34^+$ MNCs.

In conclusion, the present study demonstrated that the number of $CD34^+$ MNCs was decreased in severe CHF and increased in proportion to the amelioration of CHF during hospitalization. These findings suggest that impaired EPC recruitment might be involved in the pathophysiology of severe CHF and that a method of increasing $CD34^+$ MNCs may be a novel therapeutic strategy in severe CHF.

Acknowledgement

This study was supported in part by a grant from the Ministry of Education, Culture, Sports, Science, and Technology of Japan (15590769), Tokyo, Japan.

References

[1] Asahara T, Murohara T, Sullivan A, et al. Isolation of putative progenitor endothelial cells for angiogenesis. Science 1997;275:964–7.
[2] Bhattacharya V, McSweeney PA, Shi Q, et al. Enhanced endothelialization and microvessel formation in polyester grafts seeded with CD34(+) bone marrow cells. Blood 2000;95:581–5.
[3] Shi Q, Rafii S, Wu MH, et al. Evidence for circulating bone marrow-derived endothelial cells. Blood 1998;92:362–7.
[4] Takahashi T, Kalka C, Masuda H, et al. Ischemia- and cytokine-induced mobilization of bone marrow-derived endothelial progenitor cells for neovascularization. Nat Med 1999;5:434–8.
[5] Carmeliet P. Mechanisms of angiogenesis and arteriogenesis. Nat Med 2000;6:389–95.
[6] Hill JM, Zalos G, Halcox JP, et al. Circulating endothelial progenitor cells, vascular function and cardiovascular risk. N Engl J Med 2003;348:593–600.
[7] Gill M, Dias S, Hattori K, et al. Vascular trauma induces rapid but transient mobilization of $VEGFR2^+AC133^+$ endothelial precursor cells. Circ Res 2001;88:167–74.
[8] Shintani S, Murohara T, Ikeda H, et al. Mobilization of endothelial progenitor cells in patients with acute myocardial infarction. Circulation 2001;103:2776–9.
[9] Asahara T, Masuda H, Takahashi T, et al. Bone marrow origin of endothelial progenitor cells responsible for postnatal vasculogenesis in physiological and pathological neovascularization. Circ Res 1999;85:221–8.
[10] Murohara T, Ikeda H, Duan J, et al. Transplanted cord blood-derived endothelial precursor cells augment postnatal neovascularization. J Clin Invest 2000;105:1527–36.
[11] Tateishi-Yuyama E, Matsubara H, Murohara T, et al. Therapeutic angiogenesis for patients with limb ischaemia by autologous transplantation of bone-marrow cells: a pilot study and a randomised controlled trial. Lancet 2002;360:427–35.
[12] Inaba S, Egashira K, Komori K. Peripheral-blood or bone-marrow mononuclear cells for therapeutic angiogenesis? Lancet 2002;360:2083.
[13] Ho KK, Anderson KM, Kannel WB, et al. Survival after the onset of congestive heart failure in Framingham Heart Study subjects. Circulation 1993;88:107–15.
[14] Agnoletti L, Curello S, Bachetti T, et al. Serum from patients with severe heart failure downregulates eNOS and is proapoptotic: role of tumor necrosis factor-alpha. Circulation 1999;100:1983–91.
[15] Schiller NB, Acquatella H, Ports TA, et al. Left ventricular volume from paired biplane two-dimensional echocardiography. Circulation 1979;60:547–55.
[16] Sutherland DR, Anderson L, Keeney M, et al. The ISHAGE guidelines for $CD34^+$ cell determination by flow cytometry. J Hematother 1996;5:213–26.
[17] Hojo Y, Ikeda U, Zhu Y, et al. Expression of vascular endothelial growth factor in patients with acute myocardial infarction. J Am Coll Cardiol 2000;35:968–73.
[18] Omland T, Aakvaag A, Bonarjee VV, et al. Plasma brain natriuretic peptide as an indicator of left ventricular systolic function and long-term survival after acute myocardial infarction. Comparison with plasma atrial natriuretic peptide and N-terminal proatrial natriuretic peptide. Circulation 1996;93:1963–9.
[19] Nonaka-Sarukawa M, Yamamoto K, Aoki H, et al. Increased urinary 15-F2t-isoprostane concentrations in patients with non-ischaemic congestive heart failure: a marker of oxidative stress. Heart 2003;89:871–4.
[20] Heeschen C, Aicher A, Lehmann R, et al. Erythropoietin is a potent physiologic stimulus for endothelial progenitor cell mobilization. Blood 2003;102:1340–6.
[21] Yoon YS, Johnson IA, Park JS, et al. Therapeutic myocardial angiogenesis with vascular endothelial growth factors. Mol Cell Biochem 2004;264:63–74.
[22] Kocher AA, Schuster MD, Szabolcs MJ, et al. Neovascularization of ischemic myocardium by human bone-marrow-derived angioblasts prevents cardiomyocyte apoptosis, reduces remodeling and improves cardiac function. Nat Med 2001;7:430–6.
[23] Quaini F, Urbanek K, Beltrami AP, et al. Chimerism of the transplanted heart. N Engl J Med 2002;346:5–15.
[24] Iversen PO, Woldbaek PR, Tonnessen T, et al. Decreased hematopoiesis in bone marrow of mice with congestive heart failure. Am J Physiol Regul Integr Comp Physiol 2002;282:R166–72.

Please cite this article as: Mutsuko Nonaka-Sarukawa et al., Circulating endothelial progenitor cells in congestive heart failure ☆, International Journal of Cardiology (2006), doi:10.1016/j.ijcard.2006.07.191

Nitric oxide plays a critical role in suppression of T-cell proliferation by mesenchymal stem cells

Kazuya Sato,[1] Katsutoshi Ozaki,[1] Iekuni Oh,[1] Akiko Meguro,[1] Keiko Hatanaka,[1] Tadashi Nagai,[1] Kazuo Muroi,[1] and Keiya Ozawa[1]

[1]Division of Hematology, Jichi Medical University, Tochigi, Japan

The molecular mechanisms by which mesenchymal stem cells (MSCs) suppress T-cell proliferation are poorly understood, and whether a soluble factor plays a major role remains controversial. Here we demonstrate that the T-cell–receptor complex is not a target for the suppression, suggesting that downstream signals mediate the suppression. We found that Stat5 phosphorylation in T cells is suppressed in the presence of MSCs and that nitric oxide (NO) is involved in the suppression of Stat5 phosphorylation and T-cell proliferation. The induction of inducible NO synthase (NOS) was readily detected in MSCs but not T cells, and a specific inhibitor of NOS reversed the suppression of Stat5 phosphorylation and T-cell proliferation. This production of NO in the presence of MSCs was mediated by CD4 or CD8 T cells but not by CD19 B cells. Furthermore, inhibitors of prostaglandin synthase or NOS restored the proliferation of T cells, whereas an inhibitor of indoleamine 2,3-dioxygenase and a transforming growth factor–β–neutralizing antibody had no effect. Finally, MSCs from inducible NOS$^{-/-}$ mice had a reduced ability to suppress T-cell proliferation. Taken together, these results suggest that NO produced by MSCs is one of the major mediators of T-cell suppression by MSCs. (Blood. 2007;109:228-234)

Introduction

Because mesenchymal stem cells (MSCs) differentiate into osteocytes, chondrocytes, myotubes, and adipocytes,[1-3] they are expected to become a source of cells for regenerative therapy. Also, MSCs support hematopoietic stem cell engraftment[4-9] and modulate immunologic responses by unknown mechanisms.[9-14] Here, we investigated the molecular mechanisms by which MSCs suppress T-cell proliferation.

Transforming growth factor–β (TGF-β), hepatocyte growth factor, indoleamine 2,3-dioxygenase (IDO), and prostaglandin E2 (PGE_2) have been reported to mediate T-cell suppression by MSCs.[13-15] Specifically, neutralizing antibodies against TGF-β or hepatocyte growth factor,[13] an inhibitor of IDO,[14] or an inhibitor of prostaglandin production reverse the inhibition of T-cell proliferation by MSCs.[15] In addition, some reports have shown that a soluble factor is the major mediator of suppression,[13-17] whereas some reports have demonstrated that T-cell–MSC contact is required for this suppression.[12-14,16,17] In the current study, we sought to resolve these conflicting results by using a mouse bone marrow–derived MSC system.

One candidate soluble factor for T-cell suppression is nitric oxide (NO) because it is known to inhibit T-cell proliferation.[18-25] NO is produced by NO synthases (NOSs), of which there are 3 subtypes: inducible NOS (iNOS), endothelial NOS, and neuronal NOS. Like MSCs, it has been known that macrophages suppress T-cell proliferation. This suppression was reported to be mediated by NO inhibition of Stat5 phosphorylation.[18,19] Also, MSCs were reported to produce NO when they differentiate into chondrocytes.[26] We therefore investigated whether MSCs can produce NO and whether NO is involved in their ability to suppress T-cell proliferation.

Materials and methods

Materials

N-nitro-L-arginine methyl ester (L-NAME), indomethacin, and concanavalin A (Con A) were purchased from Wako (Osaka, Japan). Con A was used at 5 μg/mL. Indomethacin was used at 5 μM. Phorbol 12-myristate 13-acetate (PMA) and ionomycin were from Sigma (St Louis, MO) and were used at concentrations of 50 ng/mL and 1 μg/mL, respectively. Antimouse CD3/CD28 beads (Dynal Biotech ASA, Oslo, Norway) were used at 10 μL per 10^6 cells. The transwell system with 1-μm pores for 12-well dishes was from BD Falcon (Franklin Lakes, NJ). Monoclonal antibodies for CD4, CD8, CD11b, CD25, CD29, CD44, CD45, CD69, Sca-1, B220, Gr-1, and interferon-γ (IFN-γ) were from BD Pharmingen (San Diego, CA). An inhibitor of IDO, 1-methyl-DL-tryptophan (1-MT), was purchased from Sigma. An antibody for TGF-β was purchased from Peprotech (Rocky Hill, NJ). Lipopolysaccharide was from Sigma.

MSCs

MSCs were obtained from wild-type or iNOS$^{-/-}$ C57BL/6 mice. Bone marrow cells were harvested from femurs and tibias by a standard flushing method[1] and then cultivated in a plastic dish in Iscove modified Dulbecco medium (Invitrogen, Carlsbad, CA) supplemented with 10% fetal calf serum (Sigma), 2 mM L-glutamine, 0.1 mg/mL streptomycin, and 100 U/mL penicillin G (Invitrogen) or in MF medium (Toyobo, Tokyo, Japan).

All primary MSCs were characterized at least once by flow cytometry and an in vitro differentiation assay. All MSCs were positive for CD29, CD44, and Sca-1, negative for CD11b, Gr-1, and CD45, and able to

Submitted February 13, 2006; accepted August 3, 2006. Prepublished online as *Blood* First Edition Paper, September 19, 2006; DOI 10.1182/blood-2006-02-002246.

The publication costs of this article were defrayed in part by page charge payment. Therefore, and solely to indicate this fact, this article is hereby marked "advertisement" in accordance with 18 USC section 1734.

differentiate into adipocytes and osteoblasts (Figure S1, available at the *Blood* website; see the Supplemental Figures link at the top of the online article). We used at least 2 independently isolated batches of MSCs. These cells can be propagated for a long time and retain their surface phenotype and capacity to differentiate for at least 4 months.

Flow cytometric analysis

Cells were incubated with Fc block (BD Pharmingen) to inhibit nonspecific binding of antibodies to Fc receptors. Next, cells were stained in FACS buffer (phosphate-buffered saline [PBS] supplemented with 10% fetal bovine serum) with antibodies for 30 minutes on ice, washed with FACS buffer, and analyzed on a BD LSR flow cytometer (Becton Dickinson, Franklin Lakes, CA). Collected data were analyzed with CELLQUEST software (Becton Dickinson).

Enzyme-linked immunosorbent assay (ELISA)

ELISA kits for mouse IFN-γ and mouse interleukin-2 (IL-2; BD Pharmingen) were used according to the manufacturer's instructions.

Selection of CD4+, CD8+, and CD19+ cells

$CD4^+$, $CD8^+$, and $CD19^+$ cells were selected using mouse CD4, CD8, and CD19 MACS beads and an autoMACS system (Miltenyi Biotech, Auburn, CA). The purity of the cells as determined by flow cytometry with antibodies against CD4, CD8, and B220 was more than 80%.

Thymidine incorporation

Splenocytes were grown in 96-well plates containing RPMI 1640 (Invitrogen) supplemented with 10% fetal calf serum (Sigma), 2 mM L-glutamine (Invitrogen), 50 μM 2-mercaptoethanol (Sigma), 0.1 mg/mL streptomycin, and 100 U/mL penicillin G (Invitrogen). During the cultivation, the cells were pulsed for the last 8 hours of culture with 1 mCi (3.7×10^7 Bq) of [^{3}H]-thymidine (Amersham Biosciences, Piscataway, NJ). After 48 hours of growth, cells were harvested with a Packard FilterMate harvester (Perkin Elmer Life Sciences, Boston, MA), transferred to a UniFilter plate (Perkin Elmer Life Sciences), and analyzed using a TopCount microplate scintillation counter (Perkin Elmer Life Sciences). In the coculture system, MSCs were γ-irradiated (30 Gy) prior to cultivation to prevent thymidine incorporation. When using the transwell system (BD Falcon), one tenth of the cells were harvested and counted because the system includes 12-well culture dishes, which contain 10-fold more cells than the wells of a 96-well plate.

Western blot analysis

Polyclonal antibodies to phosphorylated Stat5 (Cell Signaling Technology, Danvers, MA), Stat5 (Santa Cruz Biotechnology, Santa Cruz, CA), cyclin D2 (Cell Signaling Technology), and Kip1 (Cell Signaling Technology) were used for Western blotting. Cells were lysed on ice for 15 minutes with a buffer consisting of 50 mM Tris (pH 7.5), 150 mM NaCl, 0.5% NP40, Complete proteinase inhibitor cocktail (Roche Diagnostics, Mannheim, Germany), and 1 mM Na_3VO_4. Lysates were centrifuged at 13 000*g* for 15 minutes, and supernatants were subjected to sodium dodecyl sulfate–polyacrylamide gel electrophoresis (SDS-PAGE). Proteins were transferred from the gel to a PVDF membrane (Invitrogen), and Western blotting was performed using enhanced chemiluminescence reagents (Pierce, Rockford, IL) to visualize the immunoreactive proteins.

Assay for NO production

NO is quickly converted to NO_2 and NO_3 in culture medium. Because of the presence of NO_3 in RPMI medium, we measured NO_2 production using a Griess reagent kit (Wako).

Detection of iNOS expression

Total RNA was prepared using an RNeasy kit (Qiagen, Valencia, CA) and 1 μg was reverse-transcribed using a First Strand Synthesis Kit (Invitrogen), and one tenth of the product was subjected to PCR using the following primers: for iNOS, 5′-GAGATTGGAGTTCGAGACTTC-3′ and 5′-TGGCTAGTGCTTCAGACTTC-3′; and for β-actin, 5′-CCATCATGAAGTGTGACGTTG-3′ and 5′-GTCCGCCTAGAAGCACTTGCG-3′.

Western blotting was performed using a polyclonal antibody for iNOS (BD Transduction Laboratories, Lexington, KY) or a monoclonal antibody for β-actin (Sigma) to confirm equal loading. Immunofluorescence was carried out using the polyclonal iNOS antibody (BD Transduction Laboratories) followed by Alexa Fluor 488 goat anti–rabbit IgG (Molecular Probes, Eugene, OR). To distinguish splenocytes from MSCs, cells were simultaneously stained with phycoerythrin-conjugated anti-CD45 monoclonal antibody (BD Pharmingen). Cells were fixed with ProLong Gold antifade reagent (Molecular Probes) and were visualized by confocal microscopy (Nikon, Tokyo, Japan), and images were analyzed with the accompanying confocal image analysis software (Bio-Rad, Hercules, CA).

Intracellular staining

Intracellular staining was performed using a BD Cytofix/Cytoperm kit (BD Pharmingen) according to the manufacturer's instructions.

Mice

Wild-type mice (C57BL/6) were purchased from Clea Japan (Tokyo). The $iNOS^{-/-}$ mice (C57BL/6 background) were purchased from Jackson Laboratory (Bar Harbor, ME).

Cell lines

RAW264.7 mouse macrophage cells were a generous gift from Dr Matsuura (Jichi Medical University, Tochigi, Japan). HeLa human cervical carcinoma cells were used as negative control for iNOS expression.

Statistical analysis

We used the Student *t* test for statistical analysis. Differences were considered statistically significant at P values less than .05.

Results

Characteristics of T-cell suppression by MSCs

Although many reports[9-17,27] have shown that MSCs suppress T-cell proliferation, the molecular mechanisms and the signaling molecules inhibited by MSCs have not been defined. We therefore investigated the status of activated T cells in the presence of MSCs. The expression of activation markers and the production of IL-2 and IFN-γ were evaluated by flow cytometry, ELISA, and intracellular staining. The expression of the activation markers CD25 and CD69 on CD4 or CD8 T cells was not changed by the presence of MSCs (Figure 1A). In addition, MSCs suppressed the production of IFN-γ but not IL-2 (Figure 1B, upper panel). Also, IFN-γ production was diminished after 24 hours in the presence of MSCs (Figure 1B, lower panel). These findings are in agreement with previous results,[27] but they do not explain the strong suppression of T-cell proliferation by MSCs; for example, thymidine incorporation by T cells is reduced more than 10-fold in the presence of MSCs (data not shown).

We next induced T-cell proliferation using a combination of PMA and ionomycin, which act downstream of the T-cell–receptor complex by activating protein kinase C and inducing Ca^{2+} influx, respectively. This proliferation was suppressed by MSCs (Figure 1C), suggesting that the T-cell receptor complex is not a target for the suppression and that MSCs influence signals downstream of protein kinase C and Ca^{2+} influx. As demonstrated in Figure 1C, the proliferation of both purified CD4 and CD8 T cells as well as unfractionated splenocytes was suppressed by MSCs.

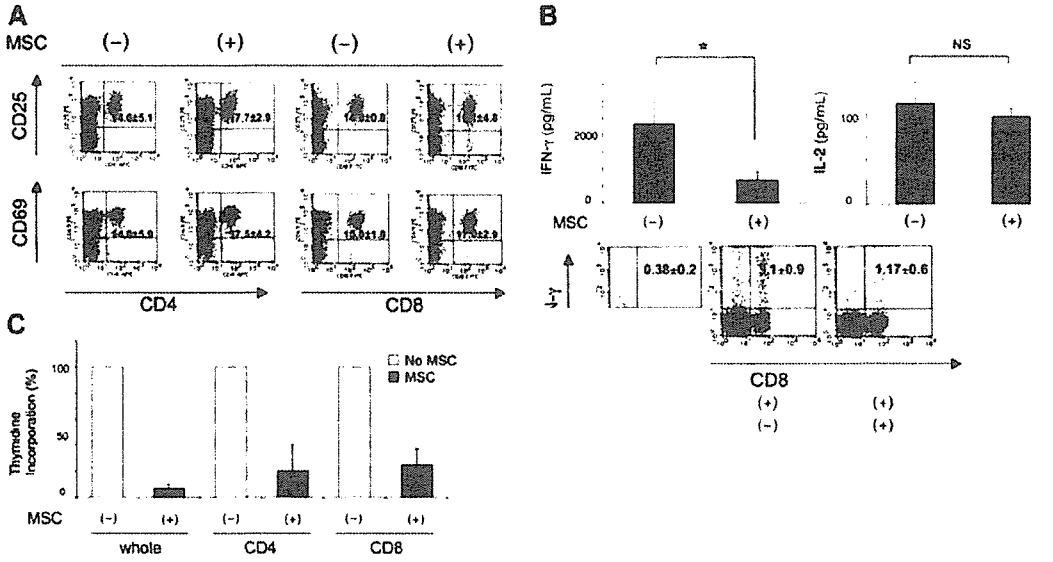

Figure 1. Status of activated T cells in the presence of MSCs. (A) Expression of the T- of splenocytes (1×10^6 cells) in a 12-well dish with anti-CD3/CD28 beads (10 μL) in the p the percentage ± the standard deviation (SD). (B) Top panel, cytokine production in the hours by ELISA. The values are the means ± SD from 3 independent experiments. Bottc the last 8 hours. The values are the mean percentages of CD8/IFN-γ–positive cells ± $CD8^+$ T-cell proliferation by PMA and ionomycin. Splenocytes (1×10^5), $CD4^+$ cells ($1 \times$ MSCs (1×10^4) in the wells of a 96-well plate. The incorporation of [^{3}H]-thymidine is st independent experiments. *$P < .05$. NS indicates $P > .05$. CD25 and CD69 on CD4 or CD8 cells 24 hours after stimulation 1×10^5 MSCs. The numbers in the top right quadrants indicate nel A. Concentrations of IL-2 and IFN-γ were determined at 48 aining of IFN-γ at 24 hours. GolgiStop (monensin) was used for t experiments. (C) MSCs suppress the induction of $CD4^+$ and $\times 10^5$) were stimulated in the presence or absence of irradiated he absence of MSCs. The values are the means ± SD from 3

Stat5 phosphorylation is inhibited by MSCs

Although T cells from Stat5ab$^{-/-}$ mice do not proliferate upon stimulation with anti-CD3, they up-regulate CD25.[28] Because this phenotype is similar to the status of activated T cells in the presence of MSCs (Figure 1A), we hypothesized that they suppress Stat5 phosphorylation. Indeed, as shown in Figure 2, Stat5 phosphorylation was diminished in activated T cells in the presence of MSCs despite equivalent IL-2 production (Figure 1B). The reported changes in cell-cycle–related proteins, including the down-regulation of cyclin D2 and up-regulation of p27 Kip1 in the presence of MSCs,[27] were observed less consistently; in most cases, we found that MSCs up-regulated cyclin D2 and down-regulated p27 Kip1 in activated splenocytes compared with freshly isolated splenocytes (data not shown).

Dose dependency and time course of NO production

Macrophages have been reported to suppress T-cell proliferation[19-23] due to the production of NO and its inhibition of Stat5 phosphorylation.[18,19] This prompted us to examine the production

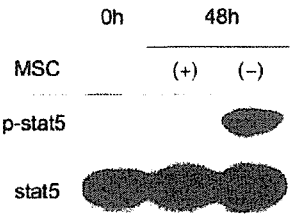

Figure 2. Inhibition of Stat5 phosphorylation in the presence of MSCs. Western blot analysis of Stat5 phosphorylation. Splenocytes (2×10^6) were activated with anti-CD3/CD28 beads in the presence or absence of 1×10^5 MSCs. After 48 hours, splenocytes were collected, lysed, and analyzed by Western blotting. Each lane contains 20 μg protein. Western blotting with anti-Stat5 is shown as a loading control. Shown are representative results from more than 5 experiments.

use MSC system. We found that MSCs caused a ıse-dependent production of NO (Figure 3A). NO ɔcted approximately 12 hours after the activation presence of MSCs. In the transwell system, in were separated from the MSCs by a 1-μm-pore roduction was initially detected approximately 24 tivation of T cells (Figure 3B).

ɔn and NO

Significant amounts of NO were not produced by MSCs cocultured with T cells in the absence of Con A or by Con A–treated MSCs or T cells (Figure 4A). In the presence of a direct interaction between T cells and MSCs, there was a high level of NO production accompanied by a strong suppression of T-cell proliferation (Figure 4A-B). In contrast, both NO production and T-cell suppression were reduced in a transwell system (Figure 4A-B). We further examined whether such a difference is observed using the RAW264.7 macrophage cell line, a well-characterized producer of NO. As with MSCs, T-cell suppression and NO production were inhibited in the transwell system using the RAW264.7 cells (Figure 4B, right side, and data not shown), suggesting that the difference reflects common aspects of T-cell suppression by NO.

T cells but not B cells induce NO

We next asked which cell type causes the NO production. We found that purified $CD4^+$ and $CD8^+$ T cells induce similar degrees of T-cell suppression as unfractionated splenocytes (Figure 1C). Therefore, it is not surprising that they also produce NO in the presence of MSCs (Figure 4C). Although MSCs suppress B-cell proliferation (~50%; data not shown), purified $CD19^+$ B cells did not appear to induce NO production in the presence of MSCs, suggesting that the mechanisms of B-cell and T-cell suppression are different.

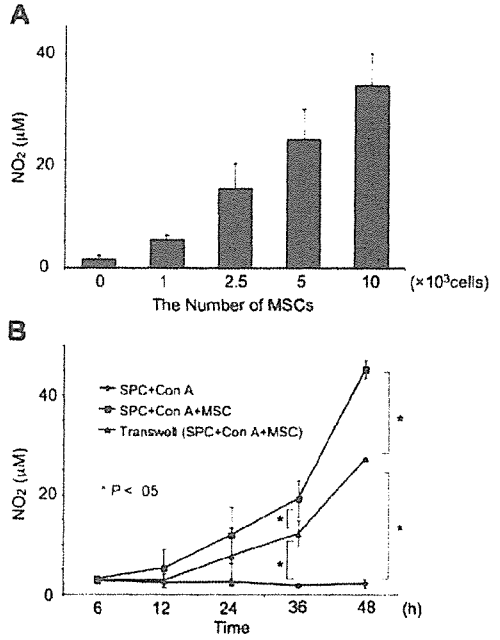

Figure 3. NO production in the presence of MSCs. (A) Dose-dependent effect of MSCs on NO production. Splenocytes (1×10^6) were activated with Con A (5 μg/mL) in the presence of the indicated number of MSCs for 48 hours in a 12-well dish. The concentrations of NO were determined by Griess assay. (B) Time course of NO production. MSCs (1×10^5/well) were treated as in panel A for the indicated amount of time. "Transwell" indicates experiments performed in 12-well dishes in which the T cells were separated from MSCs by a 1-μm-pore membrane. Values represent the means ± SD from 3 independent experiments. $^*P < .05$.

MSC–T-cell interaction and NO production

There are 2 possible explanations for the difference in NO production in the presence and absence of the transwell system. First, it is possible that there is a difference in the time course of NO production in the 2 systems. In the transwell system, a significant level of NO was typically detected after 24 hours, whereas NO production was detected after 12 to 18 hours in the presence of a direct interaction. Thus, the amount of NO produced in the transwell system was always lower than that in the presence of a direct interaction (Figure 3B). These findings suggest that a direct interaction is critical for the early and efficient production of NO as well as for the strong suppression of T-cell proliferation. A second possible explanation for the different results obtained in the transwell and direct interaction systems is that, because NO is highly unstable, in the transwell system it can lose its activity before it influences T cells.

MSCs are a producer of NO

If this second explanation is correct, MSCs should be the main producer of NO. Therefore, we examined whether MSCs can produce NO. It is known that there are 3 NO synthases (iNOS, endothelial NOS, and neuronal NOS), and only one of these, iNOS, can be induced by cell stimulation.[29] Therefore, we suspected that iNOS is induced in either T cells or MSCs. Reverse transcriptase–polymerase chain reaction (RT-PCR) (Figure 5A), Western blot analysis (Figure 5B), and immunofluorescence (Figure 5C) detected the induction of iNOS in MSCs cocultured with activated splenocytes but not in MSCs alone, splenocytes alone, or HeLa cells. The immunofluorescence studies showed that iNOS was exclusively expressed by large adherent $CD45^-$ cells, which correspond to MSCs (Figure 5C). In addition, iNOS appeared to be expressed throughout the cytoplasm as previously found in Kupffer cells and hepatocytes (Figure 5C).[30]

Specific inhibitor of NOS restores T-cell proliferation and Stat5 phosphorylation

Next, we investigated the effects of L-NAME, a specific inhibitor of NOS. As expected, L-NAME dose-dependently inhibited the production of NO by MSCs in the presence of activated T cells (Figure S2). Importantly, L-NAME restored T-cell proliferation (Figure 6A, left panel). The effect of L-NAME was dose dependent and more efficient when lower numbers of MSCs were used (Figure 6A, right panel). Using 2.5×10^3 MSCs, 1 mM L-NAME resulted in up to an approximately 80% recovery compared with the positive control (Figure 6A, left panel), suggesting that NO is one of the most important factors for T-cell suppression under the stringent conditions of our assays. On the other hand, even under these conditions, 100% recovery was not achieved, implying that other factors also contribute to the suppression of T-cell proliferation by MSCs.

L-NAME restored not only T-cell proliferation but also Stat5 phosphorylation (Figure 6B), indicating that NO inhibits Stat5 phosphorylation. Because Stat5 is required for T-cell division,[28] we suspect that NO first inhibits Stat5 phosphorylation, which then results in arrest of the cell cycle.

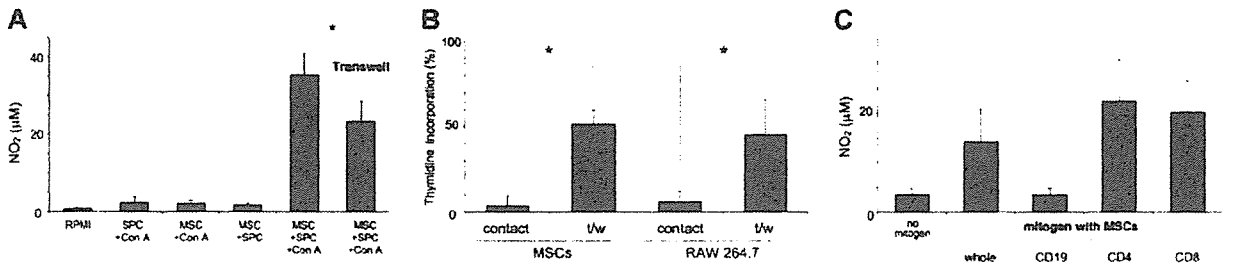

Figure 4. Relationship between NO production and T-cell suppression. (A) Production of NO. Splenocytes (1×10^6) were incubated with or without Con A in the presence or absence of MSCs for 48 hours. "Transwell" indicates experiments performed in 12-well dishes in which the T cells were separated from MSCs by a 1-μm-pore membrane. The values are the means ± SD from 3 independent experiments. $^*P < .05$. (B) T-cell proliferation in the presence or absence of the transwell system. Splenocytes (1×10^6) were activated with Con A in the presence or absence of 1×10^5 MSCs or RAW264.7 cells for 48 hours with or without the transwell. The incorporation of [^{3}H]-thymidine is shown relative to that in the absence of MSCs. The values are the means ± SD from 3 independent experiments. $^*P < .05$. (C) T cells but not B cells induce NO production. Purified CD4 or CD8 T cells (1×10^5; ~80% purity) induce NO in the presence of MSCs (1×10^4), whereas purified CD19 B cells (1×10^5; ~95% purity) do not induce significant NO production. The mitogen for T cells was Con A, and for B cells, it was lipopolysaccharide (1 μg/mL). The values are the means ± SD from 3 independent experiments. $^*P < .05$.